

A unified theory for charge-carrier transport in organic crystals

Yuan-Chung Cheng and Robert J. Silbey^{a)}

Department of Chemistry and Center for Materials Science and Engineering, Massachusetts Institute of Technology, Cambridge, Massachusetts 02139, USA

(Received 7 December 2007; accepted 12 February 2008; published online 20 March 2008)

To characterize the crossover from bandlike transport to hopping transport in molecular crystals, we study a microscopic model that treats electron-phonon interactions explicitly. A finite-temperature variational method combining Merrifield's transformation with Bogoliubov's theorem is developed to obtain the optimal basis for an interacting electron-phonon system, which is then used to calculate the bandlike and hopping mobilities for charge carriers. Our calculations on the one dimensional (1D) Holstein model at $T=0$ K and finite temperatures show that the variational basis gives results that compared favorably to other analytical methods. We also study the structures of polaron states at a broad range of parameters including different temperatures. Furthermore, we calculate the bandlike and hopping mobilities of the 1D Holstein model in different parameters and show that our theory predicts universal power-law decay at low temperatures and an almost temperature independent behavior at higher temperatures, in agreement with experimental observations. In addition, we show that as the temperature increases, hopping transport can become dominant even before the polaron state changes its character. Thus, our result indicates that the self-trapping transition studied in conventional polaron theories does not necessarily correspond to the bandlike to hopping transition in the transport properties in organic molecular crystals. Finally, a comparison of our 1D results with experiments on ultrapure naphthalene crystals suggests that the theory can describe the charge-carrier mobilities quantitatively across the whole experimental temperature range. © 2008 American Institute of Physics. [DOI: 10.1063/1.2894840]

I. INTRODUCTION

Recently, advances in preparing ultrapure single crystals of organic molecular materials have opened a new research area for material scientists. Novel electronic devices based on organic materials, such as organic light-emitting diodes, organic solar cells, and organic field-effect transistors, have been realized and proven to offer as potential substitutes for their inorganic counterparts.¹⁻³ In addition, these new experimental results have renewed the interest in developing theoretical models to better understand the intrinsic charge transport mechanisms in organic molecular crystals.⁴ The temperature dependence of charge-carrier mobilities in organic molecular crystals exhibits a universal power-law behavior (resembling the band transport found in conventional silicon-based semiconductors) at low temperatures and an almost temperature independent or slightly thermally activated behavior (resembling the hopping transport found in disordered materials) at high temperatures. The crossover from bandlike to hopping transport in the intrinsic mobilities of ultrapure organic aromatic molecular crystals occurs around room temperature.^{2,5-9} Because having high mobilities is essential for the efficiencies and fast response times of electronic devices, finding organic materials with high intrinsic charge mobilities at room temperature has been the focus of recent developments in optimizing the performance of organic-based devices.^{4,10,11} In order to describe the experimental temperature dependence of charge mobilities and de-

vised design rules that facilitate the development of organic electron devices, a theoretical model that describes both the bandlike regime and the hopping regime of charge mobilities in organic crystals is essential.

It is well known that electron-phonon interactions play a central role in the intrinsic transport properties of organic molecular crystals (OMCs). Generally speaking, the exciton and charge-carrier transport in OMC are governed by (1) the width of the electronic band (Δ , determined by resonance transfer integrals between electronic states), (2) the mechanisms and strength of electron-phonon couplings (g), (3) the characteristics of the phonon bands (e.g., phonon frequency ω_0 and widths of phonon bands), and (4) temperature (T). The complexity of the vibrations and the absence of any clear ordering of the parameters make the description of charge-carrier transport in OMC a extremely complicated problem. The situation is more complex for wide-band materials because the effective bandwidth Δ of the charge carriers can crossover from $\Delta \gg \omega_0$ at low temperatures to $\Delta \ll \omega_0$ at high temperatures due to the polaronic band narrowing effect.¹²⁻¹⁴ Therefore, the development of wide-band materials has necessitated the development of a unified theory that is applicable in all parameter regimes.

Theories constructed for a particular picture of transport have been successful in specific regimes of electron-phonon coupling strengths; however, a general description that is applicable in all parameter regimes is still unavailable. Early phenomenological transport theories, including band theory,¹⁵ stochastic Liouville equation model,¹⁶⁻¹⁹ and polaron effective mass model,⁹ have been successfully applied

^{a)}Electronic mail: silbey@mit.edu.

to many related problems, but all of them were restricted in scope and failed to provide a complete description in the light of the recent discoveries in experiments on ultrapure crystals.^{2,6,9} Recently, Troisi and Orlandi²⁰ and Hultell and Stafstrom²¹ considered charge transport in OMC by treating the vibrations classically and then numerically solving the time-dependent Schrödinger equation. Their calculations successfully reproduced the trend of temperature dependent charge-carrier mobility in OMC. However, because the vibrations are treated classically, both of their theories have the same limitations as the semiclassical stochastic Liouville approach,^{18,19,22} and can only be valid at high temperatures where the thermal energy is larger than the average phonon frequency. Clearly, a complete understanding of the problem of charge transport in OMC can be obtained only from a microscopic theory that treats the whole Hamiltonian self-consistently.

Microscopic models that explicitly include the electron-phonon interactions in the Hamiltonian seem to offer more promising results. In particular, a microscopic model first given by Holstein²³ has been examined extensively by many authors to describe charge-carrier and exciton transport,^{24–28} and to consider energy transfer between molecules embedded in a lattice.²⁹ These models are capable of reproducing both weak-coupling and strong-coupling results, but their applicability in the intermediate coupling regime is still not clear. Generally speaking, all theoretical calculations have so far failed to provide the correct magnitudes and temperature dependence of the charge-carrier mobilities in organic molecular crystal systems.^{5,9,30}

Yarkony–Silbey’s (YS) variational approach^{25,31} to exciton transport in OMC offered a promising direction to the solution of the problem because, in principle, the variational method can provide the optimal partition between the zeroth-order Hamiltonian and the perturbation, hence making the perturbation expansion in the intermediate coupling regime justified. Recently, Parris and Kenkre have extended the YS variational method to treat two phonon bands in three spatial dimensions.¹³ They argued that two phonon bands, one that narrows the band while the other scatters the electron, are required to describe the temperature dependence of charge-carrier mobilities in OMC. However, the YS variational *ansatz* contains only one variational variable and is known to suffer from a lack of flexibility.³² Therefore, a more flexible *ansatz* is necessary to obtain the correct temperature dependence of mobilities.

In this paper, we develop a microscopic model that describes quantitatively the crossover from the coherent bandlike regime to the incoherent hopping regime in a single unified theory. In Sec. II, we will describe the finite-temperature variational method and the model Hamiltonian used in this study and derive expressions that are necessary for calculating the charge-carrier mobilities in OMC. To demonstrate the improvement that a variational basis provides, in Sec. III, we will employ a simplified version of the variational method and time-independent second-order perturbation theory to study the one dimensional (1D) Holstein model at 0 K and compare the results to those from previous studies. In Sec. IV, we will apply the full variational ap-

proach of Sec. II to a 1D interacting electron-phonon system to examine the nature of polaron states in different parameter regimes and study the temperature dependence of both bandlike and hopping transport. Then, in Sec. V, we compare our results to experiments on the temperature dependent charge-carrier mobilities in ultrapure naphthalene crystals to show that the theoretical description provides quantitative agreement for both hole and electron mobilities in naphthalene crystals. Finally, in Sec. VI we briefly summarize our conclusions and remarks.

II. THEORETICAL MODELS

In this section, we present the theoretical model that is developed to describe the charge transport in molecular crystals. We first show that the Bogoliubov’s theorem on the upper bound on the free energy of a quantum system can be used as the foundation of a variational method and describe the Holstein Hamiltonian and Merrifield’s transformation that we used to model an excess charge carrier in OMC. We then combine the Bogoliubov’s bound and Merrifield’s transformation to calculate the optimal polaron state for an interacting electron-phonon system. In the end of this section, we consider a formula for charge-carrier mobilities that describes both bandlike and hopping transport and derive expressions that can be used to compute mobilities based on the optimal polaron state obtained from the variational method.

A. Bogoliubov’s bound on the free energy

We first describe our formulation for an upper bound on the free energy of a general electron-phonon system. The Helmholtz free energy A for a system defined by a Hamiltonian H at temperature T is given by

$$A_H = -\beta^{-1} \ln \text{Tr} e^{-\beta H}, \quad (1)$$

where $\beta = k_B T$. For general interacting electron-phonon systems, explicit calculation of the free energy is a formidable task. Fortunately, the following inequality exists as a consequence of the convexity of the exponential function.

Bogoliubov’s theorem. If H and H' are two self-adjoint operators with the property that the traces $\text{Tr}\{\exp(-\beta H)\}$ and $\text{Tr}\{\exp(-\beta H')\}$ are finite for all $\beta > 0$, then one has, for all $\beta > 0$,

$$\begin{aligned} -\beta^{-1} \ln \text{Tr} e^{-\beta H} &\leq -\beta^{-1} \ln \text{Tr} e^{-\beta H'} + \langle H - H' \rangle_{H'} \\ &\equiv A_H^B(H'), \end{aligned}$$

where the bracket $\langle \dots \rangle_{H'}$ denotes average according to the trial Hamiltonian H' ,

$$\langle H - H' \rangle_{H'} = \frac{\text{Tr}\{(H - H')e^{-\beta H'}\}}{\text{Tr} e^{-\beta H'}}.$$

Bogoliubov’s theorem provides an upper bound $A_H^B(H')$ on the free energy A_H based on a trial Hamiltonian H' . If a trial Hamiltonian that contains adjustable variational parameters is used, we can obtain the optimal choice for the partition of the Hamiltonian between a zeroth-order part and a perturbation part by minimizing the Bogoliubov’s bound with respect

to these variational parameters. Since the free energy is invariant under unitary transformations of the Hamiltonian, a systematic way to introduce a variational trial Hamiltonian is to adopt a unitary transformation that contains variational parameters. Suppose a unitary transformation U ($U^\dagger U=1$) is applied on H so that

$$\tilde{H} = U^\dagger H U \equiv \tilde{H}_0 + \tilde{V},$$

where \tilde{H}_0 is the zeroth-order part whose exponential $e^{-\beta\tilde{H}_0}$ can be evaluated, the Bogoliubov's bound becomes

$$A_H^B(\tilde{H}_0) = -\beta^{-1} \ln \text{Tr} e^{-\beta\tilde{H}_0} + \langle \tilde{V} \rangle_{\tilde{H}_0}. \quad (2)$$

Thus, based on the Bogoliubov's theorem, we construct a finite-temperature variational theory that provides temperature dependent optimal zeroth-order Hamiltonian for general electron-phonon systems. In the following, Eq. (2) will be used to compute the upper bound on the free energy of an interacting electron-phonon system.

B. The Hamiltonian and Merrifield's transformation

The Holstein model^{23,33} is widely used to describe the transport properties of OMC. The Hamiltonian includes a band of electronic excitation (electron or hole) in a perfect crystal coupled linearly to the coordinate of harmonic oscillators located at each site. For simplicity, we consider one molecule per unit cell and a narrow phonon band, i.e., Einstein's model of dispersionless phonons, which is a good description for the optical intramolecular modes in OMC. The second quantized form of the Hamiltonian in the direct space representation is given by ($\hbar=1$)

$$H = H_e + H_{\text{ph}} + H_{\text{int}}, \quad (3)$$

where

$$H_e = \sum_{n,m} J_{nm} a_n^\dagger a_m,$$

$$H_{\text{ph}} = \omega_0 \sum_n b_n^\dagger b_n, \quad (4)$$

and

$$H_{\text{int}} = g\omega_0 \sum_n a_n^\dagger a_n \cdot (b_n^\dagger + b_n). \quad (5)$$

Here a_n^\dagger (a_n) is the creation (annihilation) operator of the electronic excitation (electron or hole) at site n , ω_0 is the phonon frequency, and b_n^\dagger (b_n) is the creation (annihilation) operator of the localized phonon state at site n . Throughout this work, we assume that the position n and wavevector k are measured relative to the lattice constants, therefore the lattice constant and lattice structure of the crystal do not appear explicitly in our formulas. Hereafter, we will call the electronic excitation as "electron," but it is actually general and can be readily translate to other charge carriers or excitons. In addition, we assume that the concentration of charge carriers are small, so that we can work exclusively in the one particle subspace. The quantity J_{nm} is the transfer integral between localized electronic states at sites n and m . Because

of the translational symmetry, J_{nm} is a function of $n-m$ only, i.e., $J_{nm} \equiv J_{n-m}$.

The last term in Eq. (5) represents the electron-phonon coupling of magnitude determined by the dimensionless electron-phonon coupling constant g . We assume that the electron interacts linearly and locally to the phonon states. Note that from previous discussion, it is clear that a complete understanding of the problem can be obtained only when both local and nonlocal interactions are taken into account.⁴ Nonlocal interactions (phonon modulations on J) can be included in the Hamiltonian and treated in the same variational-perturbation approach in a consistent manner.^{27,34,35} Including nonlocal linear electron-phonon couplings likely will increase the scattering and result in lower band contribution and higher hopping contribution.³⁵ In addition, nonlocal electron-phonon couplings could also change the band shape and electronic density of states, and such effects would complicate the calculation of electronic free energies and transport properties.³⁴ Nevertheless, although the addition of nonlocal electron-phonon couplings will likely shift the bandlike to hoppinglike transition toward a lower temperature, qualitatively the temperature dependent universal transition in transport properties should be intact. Therefore, for simplicity, in this work we will only consider local electron-phonon couplings.

The electron-phonon Hamiltonian in Eqs. (3)–(5) has well-known exact solutions in two limiting cases. When the strength of electron-phonon coupling is set to zero, $g=0$, H is diagonal in the k -space of the lattice, with band energy given by $E(k) = \sum_{n' \neq 0} J_{n'} e^{ikn'}$. This representation corresponds to the free electron state and is a good zeroth-order basis in the weak-coupling regime in which the electronic couplings are stronger than electron-phonon couplings ($|J| \gg g^2\omega_0$). Therefore, when g is small, a perturbation expansion in terms of g in the k -representation is justified; this kind of approach is usually called a weak-coupling perturbation theory (WCPT), and has been widely used to describe covalent bonded or ionic solid-state systems in which electronic interactions are strong.

In the other limit where the resonance transfer integrals are set to zero ($J=0$), the Hamiltonian can be diagonalized by the small polaron transformation³³ that give rise to "dressed" small polaron states. The result is a transformed Hamiltonian diagonalized in the site representation; i.e., the Hamiltonian with $J=0$ is diagonal in the small polaron basis. Therefore, the small polaron basis is a good zeroth-order representation when the electron-phonon coupling is stronger than the resonance transfer integrals of the electronic states ($|J| \ll g^2\omega_0$). This representation is referred to as the small polaron representation and is widely applied to study the electron-phonon Hamiltonian in the strong-coupling regime, in which a perturbation expansion in terms of renormalized J in the small polaron representation is justified. This kind of approach is usually called a strong-coupling perturbation theory (SCPT).

Thus, well justified perturbation theories in both the weak-coupling and strong-coupling regimes are available and accurate. However, for intermediate coupling regime, there is no clear small parameters on which we can perform

a perturbation expansion. To obtain a reasonable zeroth-order representation in the intermediate coupling regime, we apply Merrifield's transformation,^{36,37}

$$U = e^{\{\sum_n a_n^\dagger a_n \sum_m f_m (b_{n+m} - b_{n+m}^\dagger)\}}, \quad (6)$$

where $\{f_m\}$ are real parameters to be determined variationally. Note that m labels the relative lattice site and f_m is the amplitude of the displacement to the equilibrium oscillator position at site $n+m$. For crystal structures with inversion symmetry, $f_m = f_{-m}$. The optimal transformation defined by $\{f_m\}$ may be temperature dependent because of the variational procedure. Note that when $f_m = \delta_m \cdot f$, the transformation is local and we recover YS one-parameter *ansatz*. In addition, when $f_m = \delta_m \cdot g$, we recover Holstein's small polaron transformation and the well-known small polaron results. Therefore, Merrifield's transformation can be regarded as a generalization of the small polaron transformation to include nonlocal displacement of the phonon modes around the electronic excitation.

Merrifield's transformation takes a localized electron operator to a partially dressed state that includes a phonon cloud (deformation of lattice) surrounding the electron,

$$A_n^\dagger = U^\dagger a_n^\dagger U = a_n^\dagger e^{-\sum_m f_m (b_{n+m} - b_{n+m}^\dagger)}.$$

This transformed basis can be seen as dressed states which contain electrons and their tightly bound phonon cloud. Physically, Merrifield's transformation contains nonlocal displacement of the lattice surrounding the electron and the values of f_m correspond to the amplitude of displacement from the equilibrium phonon position. Thus, the set of variational parameters $\{f_m\}$ represents the degree of dressing. For the boson operators, we obtain

$$B_n^\dagger = U^\dagger b_n^\dagger U = b_n^\dagger - \sum_m f_{n-m} \cdot a_m^\dagger a_m,$$

$$B_n = U^\dagger b_n U = b_n - \sum_m f_{n-m} \cdot a_m^\dagger a_m.$$

Substitution of these expressions into the Holstein Hamiltonian gives the transformed Hamiltonian,

$$\tilde{H} = U^\dagger H U = \tilde{H}_0 + \tilde{V}'.$$

The zeroth-order Hamiltonian \tilde{H}_0 is diagonal in the k -representation,

$$\begin{aligned} \tilde{H}_0 &= \sum_k \left[\omega_0 \cdot \left(\sum_m f_m^2 - 2gf_0 \right) + \tilde{J}_k \right] a_k^\dagger a_k + \omega_0 \sum_q b_q^\dagger b_q \\ &\equiv \tilde{H}_e + \tilde{H}_{\text{ph}}, \end{aligned} \quad (7)$$

where the energy band \tilde{J}_k is given by renormalized resonance transfer integrals,

$$\tilde{J}_k = \sum_{n,m} e^{ik(n-m)} J_{nm} \cdot \langle \theta_n^\dagger \theta_m \rangle_0,$$

with the renormalization factors at finite temperatures given by

$$\langle \theta_n^\dagger \theta_m \rangle_0 = e^{-1/2 \sum_m' (f_{m'-m} - f_{m'-n})^2 \cdot \coth(\beta\omega_0/2)}.$$

The transformed interacting term \tilde{V}' has a complicated form

$$\begin{aligned} \tilde{V}' &= \frac{1}{N} \sum_{k_1, k_2} \sum_{n,m} e^{-ik_1 n} e^{ik_2 m} \cdot J_{n,m} \cdot (\theta_n^\dagger \theta_m - \langle \theta_n^\dagger \theta_m \rangle_0) a_{k_1}^\dagger a_{k_2} \\ &+ \frac{\omega_0}{\sqrt{N}} \sum_{k,q} (g - f_q) \cdot a_{k+q}^\dagger a_k \cdot (b_q + b_{-q}^\dagger), \end{aligned} \quad (8)$$

where the angle brackets $\langle \cdots \rangle_0$ denotes thermal average over phonon states, and we have defined $f_q = \sum_m e^{iqm} f_m$, $\theta_n = e^{\sum_m f_{|n-m|} (b_m - b_m^\dagger)}$. Note that we have partitioned the transformed Hamiltonian into a pure electronic part \tilde{H}_e , a pure phonon part \tilde{H}_{ph} , and the perturbation part \tilde{V}' . In addition, we have intentionally included the \tilde{J}_k term in the zeroth-order Hamiltonian to make the average of the interactions identically zero, $\langle \tilde{V}' \rangle_0 = 0$.

By construction $\langle \tilde{V}' \rangle_0 = 0$, therefore Bogoliubov's bound is simply $A \leq -\beta \text{Tr} \exp(-\beta \tilde{H}_0) \equiv A_0$. Since the zeroth-order Hamiltonian $\tilde{H}_0 = \tilde{H}_e + \tilde{H}_{\text{ph}}$ is diagonal, Bogoliubov's bound is readily available

$$\begin{aligned} A_0 &= -\beta^{-1} \ln \text{Tr} e^{-\beta \tilde{H}_0} \\ &= -\beta^{-1} \ln \text{Tr} e^{-\beta \tilde{H}_e} - \beta^{-1} \ln \text{Tr} e^{-\beta \tilde{H}_{\text{ph}}}. \end{aligned}$$

We can further ignore the noninteresting phonon part and focus on the contribution from the dressed electronic states,

$$A_0^e = -\beta^{-1} \ln \text{Tr} e^{-\beta \tilde{H}_e} = -\beta^{-1} \ln \sum_k e^{-\beta \varepsilon_k}, \quad (9)$$

where the electronic band energy is given by

$$\varepsilon_k = \omega_0 \cdot \left(\sum_m f_m^2 - 2gf_0 \right) + \tilde{J}_k. \quad (10)$$

Note that the energy band of the dressed particle is temperature dependent. The temperature dependence comes into play through the temperature dependent variational parameters $\{f_m\}$ and the average effective transfer integral factor $\langle \theta_n^\dagger \theta_m \rangle_0$. For a system defined by a given set of parameters (J_0, ω_0, g, T) , minimizing the quantity A_0^e defined in Eq. (9) by adjusting $\{f_m\}$ enables us to find the optimal set of the dressing coefficients $\{f_m\}$ that describes the system, i.e., the optimal partially dressed polaron state. In addition, it is easy to check that minimizing A_0^e reproduces strong-coupling result ($\sim e^{-g^2 \coth(\beta\omega/2)}$) and weak-coupling result at finite temperature in large g and small g limits, respectively.

Note that we minimize the free energy contributed by the electronic subsystem, while in the YS treatment, the free energy of a subsystem with total (electron plus phonon) crystal wavevector K was minimized. Compared to their treatment, our approach is more straightforward and our expression in Eq. (9) is easier to evaluate. In addition, at nonzero temperatures, the quantity minimized in the YS treatment is swamped by phonon free energies. Because the uninteresting phonon free energy overwhelms the electronic free energy, it is difficult to implement a numerical scheme that minimizes

the free energy functional accurately in the YS theory. Generally speaking, we have extended the YS approach by using a more general variational *ansatz* and providing a more straightforward variational scheme that results in clean partition of the electronic free energy and phonon free energy.

C. Mobility

Yarkony and Silbey derived a general expression for exciton mobilities in molecular crystals that describes both bandlike and hopping transport.^{25,27} We use their expression to perform mobility calculations. In Appendix A, we summarize their derivation and the resulting mobility formula when the transformed Hamiltonian in Eqs. (7) and (8) is used.

The expression for $W_{q,q+K;k,k+K}$ in Eq. (A10) can be used to calculate the bandlike mobility μ_B and the hopping mobility μ_H . The calculation of the bandlike contribution to the electron mobility [Eq. (A6)] is more straightforward. The group velocity $v_k = \nabla_k \varepsilon_k$ and the equilibrium density matrix $\sigma_{kk}^{\text{eq}} = e^{-\beta \varepsilon_k} / \sum_q e^{-\beta \varepsilon_q}$ can be easily obtained by recalling the formula for ε_k ,

$$\varepsilon_k = \omega_0 \cdot \left(\sum_m f_m^2 - 2gf_0 \right) + \sum_{n,m} e^{ik(n-m)} J_{nm} \cdot e^{-1/2 \sum_m (f_{m'-m} - f_{m'-n})^2 \cdot \coth(\beta \omega_0 / 2)}.$$

The rate of scattering out of state k can be calculated from $W_{q,q+K;k,k+K}$ using

$$\Gamma_{kk} = \sum_q W_{q,q+K;k,k+K} |_{K=0, \alpha \rightarrow 0}.$$

Note that because of the δ -functions in the limit of $\alpha \rightarrow 0$, the summation over q can be replaced by summing $W_{q,q;k,k}$ over q points that satisfy the energy conservation conditions required by the δ -functions. In general, when the energy band ε_k is obtained, the quantities Γ_{kk} can be evaluated and the bandlike mobility can be calculated according to Eq. (A6).

In contrast, the hopping contribution to the electron mobility [Eqs. (A7) and (A8)] is difficult to evaluate. An analytical expression for γ_{kk} is unavailable even for the simplest one dimensional system. Nevertheless, with finite but small α ($0 < \alpha \ll 1$), the expression for the second derivative of $W_{q,q+K;k,k+K}$, $(d^2/dK^2) W_{q,q+K;k,k+K} |_{K=0}$ can be obtained using a computational algebraic software such as MAPLE or MATHEMATICA, and the result can be numerically integrated to obtain the hopping mobility according to Eqs. (A7) and (A8).

The expressions for the upper bound on the electronic free energy A_0^e in Eq. (9) and the relaxation tensor $W_{q,q+K;k,k+K}$ in Eq. (A10) are the main results of the present work. Minimizing A_0^e with respect to the dressing coefficients $\{f_m\}$ gives the optimal polaron state, and the optimal set of $\{f_m\}$ can then be used to compute $W_{q,q+K;k,k+K}$ and electron mobilities according to Eqs. (A5)–(A8). To demonstrate our variational-perturbation approach, we will apply this method to study the properties of a simple electron-phonon system in one spatial dimension in the following sections.

III. POLARON STATES AT 0 K

Numerous variational methods have been applied to study the Holstein Hamiltonian in the context of polaron problem.^{36,38–41} In particular, Lindenberg and co-workers^{39,42} have performed extensive investigations on several variational *Ansätze* and found that variational methods can produce results comparable to computationally much more demanding methods such as quantum Monte Carlo,^{43,44} density matrix renormalization group (DMRG), and cluster diagonalization methods. Although variational treatments of the Holstein Hamiltonian have been carried out extensively, most existing works are restricted in the ground state and focused on problems such as polaron localization and spectra properties. The number of treatments of the Holstein Hamiltonian at finite temperature or regarding dynamical properties is limited.^{45–47} Therefore, before we proceed to study the dynamics of the Holstein Hamiltonian at finite temperatures, we first examine the variational method described in Sec. II at zero temperature and compare our calculations to previous results. The objective is to test the applicability of our variational method. We will show that our variational approach combined with second-order perturbation theory produces results that are in good agreement with calculations employing more complicated methods.

We consider a 1D system with only nearest-neighbor resonance transfer integrals described by the following Hamiltonian:

$$H = J_0 \sum_n (a_n^\dagger a_{n+1} + a_{n+1}^\dagger a_n) + \omega_0 \sum_n b_n^\dagger b_n + g \omega_0 \sum_n a_n^\dagger a_n \cdot (b_n^\dagger + b_n). \quad (11)$$

To illustrate the method in the simplest form, we use Merrifield's transformation [Eq. (6)] with a dressing coefficient $f_m = f \cdot \delta_m$, i.e., we consider only a single variation parameter f . Applying the simplified unitary transformation to the 1D Hamiltonian, we obtain the transformed Hamiltonian $\tilde{H} = \tilde{H}_0 + \tilde{V}'$, where

$$\tilde{H}_0 = \sum_k [\omega_0 \cdot (f^2 - 2gf) - 2J_0 e^{-f^2} \cos k] a_k^\dagger a_k + \omega_0 \sum_q b_q^\dagger b_q \quad (12)$$

and

$$\begin{aligned} \tilde{V}' = & \frac{1}{N} \sum_{k_1, k_2} \sum_{n, m} e^{-ik_1 n + ik_2 m} J_0 \delta_{1, |n-m|} \\ & \times [e^{-f(b_n - b_n^\dagger)} e^{f(b_m - b_m^\dagger)} - e^{-f^2}] a_{k_1}^\dagger a_{k_2} \\ & + \frac{\omega_0(g-f)}{\sqrt{N}} \sum_{k, q} a_{k+q}^\dagger a_k (b_q + b_{-q}^\dagger). \end{aligned} \quad (13)$$

Therefore, the zeroth-order band structure of the 1D system can be written as

$$E^{(0)}(k) = \omega_0 \cdot (f^2 - 2gf) - 2J_0 e^{-f^2} \cos k. \quad (14)$$

At $T=0$ K, the Bogoliubov's bound in Eq. (2) is an upper bound on the energy of the ground state. For the 1D nearest-

neighbor coupling system at $T=0$ K, the optimal f satisfies

$$\frac{d}{df} E^{(0)}(k=0)|_{f=f_{\text{opt}}} = 0, \quad (15)$$

and we have the following self-consistent equation for the optimal f :

$$f_{\text{opt}} = \frac{g\omega_0}{\omega_0 + 2J_0 e^{-f_{\text{opt}}^2}}. \quad (16)$$

Given g , J_0 , and ω_0 , the optimal f_{opt} can be obtained by solving Eq. (16) iteratively. Note that the ground state energy $E^{(0)}(k=0)$ as a function of f can have more than one minima, therefore, when an iterative scheme is used to calculate f_{opt} , multiple initial guesses must be applied and then the resulting energy values compared to locate the true optimal f_{opt} .

We now calculate the second-order energy correction to the energy band structure based on the partially dressed basis defined by f_{opt} . In the $|k; \mathbf{n}\rangle$ basis set, where k denotes the k state of the electron and the vector \mathbf{n} denotes the states of all phonon modes in the system, the energy band structure calculated from second-order time-independent perturbation theory is

$$\begin{aligned} E(k) &= E^{(0)}(k) + E^{(2)}(k) \\ &= \omega_0 \cdot (f_{\text{opt}}^2 - 2gf_{\text{opt}}) - 2J_0 e^{-f_{\text{opt}}^2} \cos k \\ &\quad - \sum_{n_T \geq 0} \sum_{k'} \frac{n_i}{\varepsilon_k - \varepsilon_{k'} - n_T \omega_0} \sum_i |\langle k'; \mathbf{n}_i | \tilde{V}' | k; 0 \rangle|^2, \end{aligned} \quad (17)$$

where $n_T=0,1,2,\dots,\infty$ is the total number of phonon quanta, \mathbf{n}_i is a vector representing the distribution of n_T phonon quanta in all phonon modes, and the summation over \mathbf{n}_i means summing over all phonon configurations that contains totally n_T quanta of phonons. The $E^{(2)}(k)$ term can be evaluated analytically, and the explicit expression is given in Appendix C. In the following we will calculate ground state energy and polaron effective mass using Eqs. (14) and (17) and compare the results to other methodologies in the literatures to measure the adequacy of the variational-perturbation method.

A. Ground state energy

The ground state properties of the 1D Holstein Hamiltonian have been investigated extensively, and accurate results regarding the ground state energy of the 1D Holstein Hamiltonian are available.⁴² Therefore, we first compare our result to these calculations at zero temperature. In Table I, we compare the ground state energy from our method to a number of previous calculations for a set of system parameters in the intermediate coupling regime ($J_0/\omega_0=1$ and $g=1$). The zeroth-order ground state energy $E^{(0)}(0)$ [Eq. (14)] and the second-order result $E(0)=E^{(0)}(0)+E^{(2)}(0)$ [Eq. (17)] are listed along with results from several other methods. Among the methodologies listed in Table I, the $E^{(0)}(0)$, Merrifield,^{36,37} Toyozawa,^{38,48} and global-local³⁹ methods are variational methods, therefore, these numbers are upper bounds to the true ground state energy. Note that

TABLE I. A comparison of ground state energy of a 1D Holstein model from different theoretical methods.

$J_0/\omega_0=1, g=1$		
Value	Method	Reference
-2.3473	$E^{(0)}(0)$	This work, Eq. (14)
-2.4472	second-order WCPT	This work, Eq. (18)
-2.4561	Merrifield variation	36 and 37
-2.4687	Toyozawa variation	38 and 48
-2.4693	global-local variation	39
-2.4697	DMRG $N=32$	49
	Exact value	
-2.471	Cluster diag. $N=6$	46 and 50
-2.4826	$E(0)$	This work, Eq. (17)
-2.5679	GS second-order SCPT	This work, Eq. (19)
-3.0896	Marsiglio's second-order SCPT	53 and 73, Eq. (20)

the true bulk ground state energy is believed to lie between the $N=32$ DMRGs (Ref. 49) and the $N=6$ cluster diagonalization^{46,50} values, both of which are computationally demanding numerical methods. At this particular set of parameters, the value given by $E^{(0)}(0)$ (YS *ansatz*) significantly overestimates the ground state energy, while the other three variational methods give values that are within 1% range of the exact value. The less satisfactory result given by $E^{(0)}(0)$ is clearly due to the restricted form containing only one variational parameter in the variational *ansatz*, and the inclusion of nonlocal deformation of the lattice in Merrifield's method significantly improves the value for ground state energy. When the second-order correction is applied, the variational-perturbation result $E(0)$ gives a value that is within 1% range of the exact value at $J_0/\omega_0=1$ and $g=1$. This significant improvement compared to $E^{(0)}(0)$ indicates that the perturbation expansion based on the optimal polaron basis is justified in the intermediate coupling regime.

To compare our variational-perturbation method to other analytical theories, some approximate perturbation results are also listed in Table I. The second-order WCPT based on the free electron states is a limiting case of our method. By setting $f=0$ in Eq. (17), the band structure from the second-order WCPT is obtained

$$\begin{aligned} E^{\text{WCPT}}(k) &= -2J_0 \cos k - g^2 \omega_0^2 \frac{1}{N} \sum_{k'} \\ &\quad \times \frac{1}{2J_0 \cos k' - 2J_0 \cos k - \omega_0}. \end{aligned}$$

Near the bottom of the band where $k \sim 0$ and $\cos k \sim 1$, the integral over k' can be evaluated explicitly to give

$$\begin{aligned} E_{k \sim 0}^{\text{WCPT}}(k) &= -2J_0 \cos k - \frac{g^2 \omega_0^2}{2J_0} \\ &\quad \times \frac{1}{\sqrt{(\cos k + \omega_0/2J_0)^2 - 1}}. \end{aligned} \quad (18)$$

Grover-Silbey's second-order strong-coupling perturbation theory (GS SCPT) is the formalism first used by those authors to study exciton transport in OMC.^{51,52} The present

method also contains the GS SCPT theory in the limit of $f = g$, and the resulting band structure around the bottom of the band is

$$E_{k \sim 0}^{\text{GS}}(k) = -g^2 \omega_0 - 2J_0 e^{-g^2} \cos k - 2J_0 e^{-g^2} \sum_{n_T=1}^{\infty} \frac{f_{\text{opt}}^{2n_T}}{n_T!} \\ \times \frac{A\sqrt{A^2-1} - AB + B\sqrt{A^2-1} - A^2 - C}{\sqrt{A^2-1}},$$

$$A = \cos k + n_T \omega_0 / 2J_0 e^{-g^2},$$

$$B = \frac{1}{2}[2(-1)^{n_T} + (-2)^{n_T}] \cos k,$$

$$C = \frac{1}{2}[2^{n_T} + \cos 2k - 1]. \quad (19)$$

Finally, the result from a second-order strong-coupling perturbation theory due to Marsiglio (Marsiglio SCPT) is also listed.⁵³ Similar to the GS approach, Marsiglio's theory is also based on the small polaron transformation and treats the renormalized electronic coupling term as the perturbation. However, Marsiglio used the transformed coupling term directly and did not absorb the first order correction into the zeroth-order Hamiltonian. Thus, the first-order energy correction is nonzero in Marsiglio's theory, i.e., $\langle V \rangle_0 \neq 0$. The band structure up to the second order in J_0 from Marsiglio's SCPT is given by

$$E^M(k) = -g^2 \omega_0 - 2J_0 e^{-g^2} \cos k - 2h(g^2) \cos(2k) \\ - 2h(2g^2),$$

$$h(x) = \frac{J_0^2 e^{-2g^2}}{\omega_0} [Ei(x) - \gamma - \ln x], \quad (20)$$

where $Ei(x)$ is the exponential integral and γ is Euler's constant. Marsiglio's theory is widely used in studies of the Holstein polaron problem.

From Table I, we clearly see that all these simple perturbation theories fail badly in the intermediate coupling regime. In contrast, the present method using perturbation expansion based on a variational zeroth-order Hamiltonian successfully reproduces the ground state energy of the 1D Holstein model within a reasonable error range. Note that Table I aims at demonstrating the improvement gained by using a variational zeroth-order Hamiltonian in the intermediate coupling regime; because we only compare the results in a single point of $J_0/\omega_0=1$ and $g=1$, the trend shown in Table I is in no means representative for the quality of results from different theories.

B. Polaron effective mass

In addition to the ground state energies, we also compare polaron effective masses calculated from a number of different methods. The effective mass of a polaron band m^* can be calculated using the following formula:

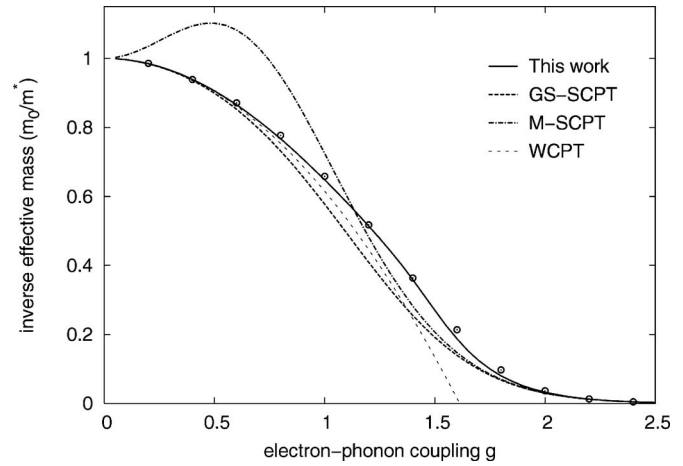


FIG. 1. Inverse effective mass at $T=0$ K for the 1D Holstein model at $J_0/\omega_0=1/2$ as a function of the electron-phonon coupling g . We show results calculated from five different theories: The variational method using Toyozawa's Ansatz (open circles), the variational-perturbation theory described in this work, a second-order strong-coupling perturbation theory based on Grover and Silbey's formulation (GS-SCPT), the second-order strong-coupling perturbation theory due to Marsiglio (M-SCPT), and second-order weak-coupling perturbation theory (WCPT). Our variational-perturbation method gives result that is in excellent agreement to Toyozawa's variational results.

$$\frac{m^*}{m_0} = \frac{2J_0}{\left. \frac{\partial^2 E(k)}{\partial k^2} \right|_{k=0}}. \quad (21)$$

Note that for the convenience of comparison, we scale the polaron effective mass by the effective mass of a free electron band $m_0=2J_0$. In Fig. 1, we show the inverse effective mass as a function of electron-phonon coupling constant g at $J_0/\omega_0=1/2$. Curves calculated from the present variational-perturbation method are shown along with results from three other second-order perturbation theories. In addition, values calculated numerically using Toyozawa's variational method are also displayed. Toyozawa's method is known to produce fairly accurate results in this parameter regime,^{38,48} therefore, values from Toyozawa's method can serve as the guideline for our comparison. In the small coupling (g) regime, the effective mass of the polaron state resembles that of a free electron, $m^*/m_0 \sim 1$; as the strength of the electron-phonon coupling increases, the polaron effective mass grows monotonically, and eventually follows the e^{-g^2} behavior predicted by SCPT theories at strong couplings ($g \gg 1$). Note that in the intermediate coupling regime, the effective mass grows rapidly, indicating a change in the character of the polaron state from a weakly dressed state to a fully dressed state. We will discuss this transition in more details later and focus solely on the comparison of different theoretical methods here.

The applicabilities of the second-order WCPT and Marsiglio's second-order SCPT methods are clearly restricted to the weak-coupling and strong-coupling regimes, respectively; in particular, both of them fail badly in the intermediate coupling regime. Note that at small g , Marsiglio's strong-coupling theory results in effective masses that are smaller than m_0 , $m_{M\text{-SCPT}}^* < m_0$, which is unphysical. In con-

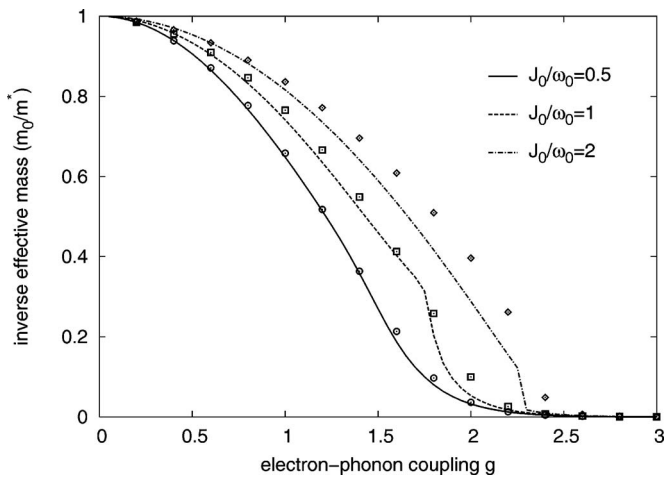


FIG. 2. Inverse effective mass at $T=0$ K for the 1D Holstein model as a function of the electron-phonon coupling g . Curves calculated using the present variational-perturbation theory at $J_0/\omega_0=1/2, 1$, and 2 are shown along with results from Toyozawa's variational method. At smaller J_0 , our variational-perturbation method is in excellent agreement to Toyozawa's variational results. At larger J_0 , our variational-perturbation method starts to deviate from Toyozawa's method at intermediate to large g .

trast to Marsiglio's theory, GS-SCPT describes both strong- and weak-coupling limits adequately and does not suffer the problem of giving unphysical results. In the intermediate regime, the GS-SCPT method gives correct trend, but overestimates the effective mass. A distinct feature in Grover and Silbey's theory (and the present variational-perturbation theory too) is that the average matrix elements of the perturbation term are included in the zeroth-order Hamiltonian so that the first order correction is zero. Note that our comparison in Fig. 1 clearly indicates the importance of including the first-order correction in the zeroth-order Hamiltonian.

In contrast to all other simple perturbation theories, the present variational-perturbation method is in excellent agreement with Toyozawa's method at $J_0/\omega_0=1/2$ in all electron-phonon coupling strengths. In Fig. 2, we compare our variational-perturbation method to Toyozawa's method at $J_0/\omega_0=1/2, 1$, and 2 . At smaller J_0/ω_0 , the agreement is excellent, while at larger J_0/ω_0 , the agreement is less satisfactory and the variational-perturbation method starts to deviate from Toyozawa's method at intermediate to large g . Nevertheless, the present model describes the effective mass of the 1D Holstein model quantitatively at smaller J_0/ω_0 and semiquantitatively at $J_0/\omega_0 > 1$. Note that the present method is less favorable at large J_0/ω_0 ; we believe it is due to the restricted form of the one-parameter *ansatz*. For example, at large J_0/ω_0 , nonlocal lattice deformation, which is included in more general Merrifield's transformation but not in the current one-parameter *ansatz*, is expected to be important for a description of the polaron state.

Evidently, the present variational-perturbation method gives favorable results compared to other simple perturbation theories and is capable of describing the 1D Holstein model at $T=0$ K in the intermediate coupling regime. Considering that at $T=0$ K, the present analytical method with only one variational parameter is able to give results that are in agreement with much more complicated numerical methods, we

believe applying perturbation theory based on a variational optimal basis at finite temperature would also give significantly improved results.

IV. INTERACTING EXCITON-PHONON SYSTEM IN 1D

In this section, we apply the theoretical methods we developed in Sec. II to a simple 1D system and discuss the implications of the results regarding the mobilities of charge carriers in organic molecular crystals. We investigate a simplified model with one spatial dimension and contains only nearest-neighbor transfer integrals,

$$J_{nm} = J_0 \cdot \delta_{n,m \pm 1}, \quad (22)$$

where J_0 is the bare resonance transfer integral between two nearest-neighbor sites. The phonon renormalized band structure under Merrifield's transformation is given by

$$\begin{aligned} \varepsilon_k &= \omega_0 \cdot \left(\sum_m f_m^2 - 2gf_0 \right) + \tilde{J}_k \\ &= \omega_0 \cdot \left(\sum_m f_m^2 - 2gf_0 \right) - 2J_{\text{eff}} \cos k, \end{aligned} \quad (23)$$

where we have defined the effective transfer integral renormalized by the dressing of the phonons,

$$J_{\text{eff}} = J_0 e^{-\sum_m (f_m^2 - f_m f_{m+1}) \coth(\beta\omega_0/2)}. \quad (24)$$

Note that J_{eff} is temperature dependent, and the temperature dependence of J_{eff} comes into play through the temperature dependent parameters $\{f_m\}$ and the $\coth(\beta\omega_0/2)$ factor; as a result, the temperature dependence is different from ordinary small polaronic band narrowing factor $e^{-g^2 \coth(\beta\omega_0/2)}$.

Bogoliubov's bound for the 1D system is easily obtained from Eq. (23),

$$\begin{aligned} A &\leq A_0^e = -\beta^{-1} \ln \sum_k e^{-\beta\varepsilon_k} \\ &= -\beta^{-1} \ln \left\{ e^{-\beta\omega_0(\sum_m f_m^2 - 2gf_0)} \sum_k e^{2J_{\text{eff}}\beta \cos k} \right\}. \end{aligned} \quad (25)$$

For a bulk system, we can convert the sum over k into an integral and obtain

$$A_0^e = -\beta^{-1} \ln N + \omega_0 \left(\sum_m f_m^2 - 2gf_0 \right) - \beta^{-1} \ln \{I_0(2\beta J_{\text{eff}})\}, \quad (26)$$

where N is the size of the system, and $I_0(x)$ is the Bessel function of the first kind. The extreme values of A_0^e can be found at points where equality $\partial A_0^e / \partial f_m = 0$ is satisfied for all f_m . As a result, we obtain a system of coupled equations,

$$\begin{aligned} f_m - g\delta_m + \frac{J_{\text{eff}}}{\omega_0} \times \frac{I_1(2\beta J_{\text{eff}})}{I_0(2\beta J_{\text{eff}})} \times (2f_m - f_{m+1} \\ - f_{m-1}) \cdot \coth(\beta\omega_0/2) = 0. \end{aligned} \quad (27)$$

Equation (27) is used to calculate the optimal set of $\{f_m\}$ that minimizes Bogoliubov's bound on free energy. Note that the effective transfer integral J_{eff} also depends on $\{f_m\}$, therefore, the system of equations must be solved self-consistently. Again, A_0^e as a function of $\{f_m\}$ can have more than one

minima, therefore, multiple initial guesses must be applied and then the resulting A_0^e values compared to locate the true optimal set of dressing coefficients. Nevertheless, for given g , ω_0 , β , and J_0 , it is trivial to obtain accurate solutions and select the optimal solution on a personal computer.

We now check the strong-coupling and the weak-coupling limits in Eq. (27). In the limit that $g^2\omega_0 \gg J_0$, we can neglect the last term in the right-hand side of Eq. (27) and obtain $f_m = g\delta_m$. The transformation reduces to the small polaron transformation, and we recover the conventional strong-coupling results. On the other hand, when $J_0 \gg g^2\omega_0$, the first two terms in Eq. (27) can be neglected, and the solution to the equation is $f_m = (f_{m+1} + f_{m-1})/2$. Because of the symmetry and boundary conditions required for the 1D crystal, $f_m = f_{-m}$ and $\lim_{m \rightarrow \infty} f_m = 0$, the only physically admissible solution to $\{f_m\}$ is $f_m = 0$. Thus, we also recover the weak-coupling results from Eq. (27).

In order to compute the bandlike and hopping mobilities using the results in Sec. II C, we need to calculate the equilibrium density matrix σ_{kk}^{eq} , the group velocity v_k , and the relaxation tensor elements $W_{q,q+K;k,k+K}$ for the 1D system. Both σ_{kk}^{eq} and v_k can be evaluated easily from the band structure in Eq. (23) to yield

$$\sigma_{kk}^{\text{eq}} = \frac{1}{N} \times \frac{e^{2\beta J_{\text{eff}} \cos k}}{I_0(2\beta J_{\text{eff}})}, \quad (28)$$

$$v_k = \frac{d\varepsilon_k}{dk} = 2J_{\text{eff}} \sin k. \quad (29)$$

To compute the relaxation tensor elements $W_{q,q+K;k,k+K}$ for the 1D nearest-neighbor system, we insert $J_{nm} = J_0 \cdot \delta_{n,m \pm 1}$ into the expression for $W_{q,q+K;k,k+K}$ [Eq. (A10)] to obtain

$$\begin{aligned} W_{q,q+K;k,k+K}^{\text{1d}} = & n_0 \omega_0^2 (g^2 - f_{k-q}^2) \left[\frac{\alpha}{\alpha^2 + (\varepsilon_q - \varepsilon_k - \omega_0)^2} + \frac{\alpha}{\alpha^2 + (\varepsilon_{q+K} - \varepsilon_{k+K} - \omega_0)^2} \right] + (n_0 + 1) \omega_0^2 (g^2 - f_{k-q}^2) \\ & \times \left[\frac{\alpha}{\alpha^2 + (\varepsilon_q - \varepsilon_k + \omega_0)^2} + \frac{\alpha}{\alpha^2 + (\varepsilon_{q+K} - \varepsilon_{k+K} + \omega_0)^2} \right] + 2J_{\text{eff}}^2 \times \sum_{n=1}^{\infty} \sum_{m=0}^n \sum_{z=-\infty}^{\infty} \frac{A_z^m B_z^{n-m}}{m!(n-m)!} \{ \cos[k+q+K+(k \\ & -q)z] + (-1)^n \cos[K+(k-q)z] \} \times \left\{ \frac{\alpha}{\alpha^2 + [\varepsilon_q - \varepsilon_k + (2m-n)\omega_0]^2} + \frac{\alpha}{\alpha^2 + [\varepsilon_{q+K} - \varepsilon_{k+K} + (2m-n)\omega_0]^2} \right\}, \end{aligned} \quad (30)$$

where the functions

$$A_z = -(n_0 + 1) \sum_l [2 \cdot f_l f_{l+z} - f_l f_{l+z-1} - f_l f_{l+z+1}],$$

$$B_z = -n_0 \sum_l [2 \cdot f_l f_{l+z} - f_l f_{l+z-1} - f_l f_{l+z+1}].$$

Once the optimal set of dressing coefficients is obtained, Eq. (30) is used to evaluate the relaxation tensor elements for the 1D system, and the result is then integrated numerically according to Eqs. (A6) and (A7) to calculate the bandlike and hopping mobilities, respectively. In our numerical calculations, we use a constant phonon relaxation rate $\alpha = 0.01\omega_0$. In all parameter range we studied the result is insensitive to the value of α given that a good numerical algorithm and enough numerical points are applied to evaluate the integrals. In addition, an extra constant scattering rate $\gamma_0 = 0.001\omega_0$ is employed in our calculations for bandlike mobilities [Eq. (A6)]. The additional scattering term γ_0 is used to mimic the scattering channel due to impurities in the crystal, which is known to dominate the bandlike transport at low temperature. The amplitude of γ_0 only affects the mobility at

extremely low temperature, therefore adding the γ_0 term does not alter the crossover from bandlike to hopping transport. In the following, we first study the small polaron transition using the finite-temperature variation method, and then present our results of mobility calculations for the 1D system.

A. Small polaron transition

In this subsection, we examine the optimal polaron state, defined by the optimal set of $\{f_m\}$, from the finite-temperature Merrifield variational method for the 1D nearest-neighbor system. The dressing coefficients $\{f_m\}$ in Merrifield's *ansatz* represent the deformation of the lattice around the electron, and the extend of the deformation characterizes the nature of the polaron state. When the lattice deformation is extended over many lattice sites, the state is usually called a "large polaron" state; on the other hand, when the deformation is restricted to a single site, a "small polaron" state occurs. It is well known that at $T=0$ K, the Holstein Hamiltonian exhibits large polaron states at weak electron-phonon couplings (small g) and small polaron states

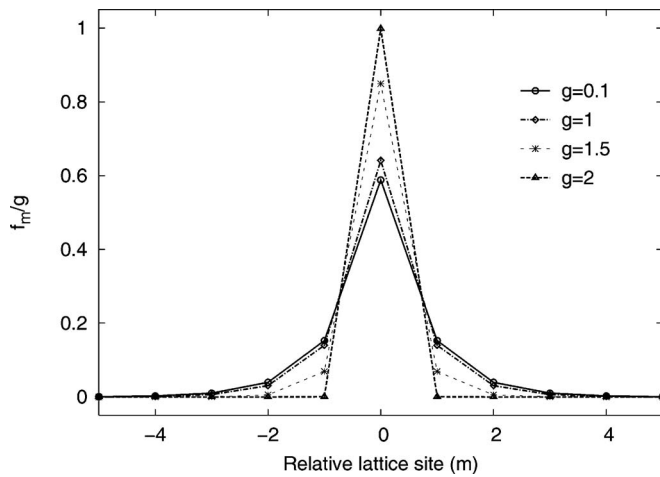


FIG. 3. Polaron profiles at $\beta\omega_0=10$ for a 1D nearest-neighbor system with $J_0/\omega_0=1/2$ at different strengths of electron-phonon couplings g . As g increases, the polaron profile becomes more localized.

at strong couplings (large g). The transition from large polaron state to small polaron state, also called the self-trapping transition, is the focus of many theoretical investigations.^{54–59} Our finite-temperature variational method allows us to examine this transition at finite temperatures.

1. Lattice deformation

We first show the structure of polaron states represented by the optimal set of dressing coefficients $\{f_m\}$ at different strengths of electron-phonon couplings (g). In Fig. 3, we show the relative amplitude of lattice deformations (f_m/g) surrounding an electron at low temperature ($\beta\omega_0=10$) for a system with reduced nearest-neighbor transfer integral $J_0/\omega_0=1/2$ at different g . At weak coupling, the deformation of lattice (polaron profile) is extended over many lattice sites and the relative amplitudes of deformations are small, therefore, the polaron state is only weakly dressed and of the character of a large polaron state. Note that the *ansatz* used by Yarkony and Silbey contains only a single variational parameter, as a result, their *ansatz* cannot describe these large polaron states adequately. As the strength of electron-phonon coupling g increases, the lattice deformation gradually becomes more localized. At $g > 1.5$, the deformation is complete localized on a single lattice site and $f_0/g \sim 1$, therefore, the polaron state is a fully dressed small polaron state. We emphasize that the “localization” is only relative to the position of an electron in the site representation, and in no means indicates a localized polaron. The polaron profile shown in Fig. 3 should be interpreted as correlations between the position of the electron and the lattice deformation; the eigenstates of the zeroth-order Hamiltonian after Merrifield’s transformation are momentum states delocalized over the whole crystal, i.e., the eigenstates form a polaron band.

To show the effect of varying temperatures, we present polaron profiles for a 1D system with $J_0/\omega_0=1/2$ and $g=1/2$ at different temperatures in Fig. 4. Clearly, the temperature of the system plays a role resembling that of the electron-phonon coupling g . As temperature increases, the

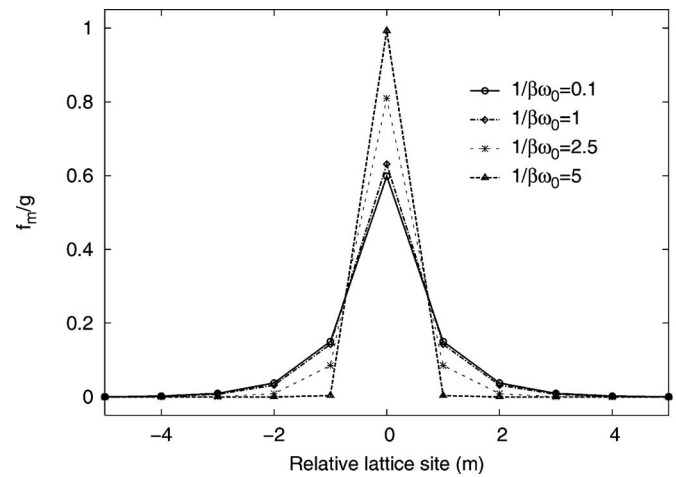


FIG. 4. Polaron profiles for a 1D nearest-neighbor system with $J_0/\omega_0=1/2$ and $g=1/2$ at different temperatures. The polaron profile becomes more localized at higher temperatures.

deformation of lattice becomes increasingly localized. Thus, increasing temperature also drives the transition from a large polaron state to a small polaron state.

2. Polaronic band narrowing effect

To further characterize the structure of the polaron states and the polaronic band narrowing effect for the 1D system, we study the effective transfer integrals J_{eff} [Eq. (24)] for optimal polaron states in a broad range of parameters. Note that for the 1D nearest-neighbor system, the bare bandwidth is $4J_0$ and the polaronic narrowed effective bandwidth is $4J_{\text{eff}}$. Hence, J_{eff} is a direct measure of the effective bandwidth of the electrons.

In Fig. 5, we show relative effective transfer integral J_{eff}/J_0 as a function of electron-phonon coupling g at a low temperature ($\beta\omega_0=10$) for 1D systems with different bare transfer integrals. The transition from a weakly dressed large polaron state at small g ($J_{\text{eff}}/J_0 \approx 1$) to a strongly dressed small polaron state at large g ($J_{\text{eff}}/J_0 \ll 1$) can be clearly seen. A rapid decrease in J_{eff} occurs in the intermediate cou-

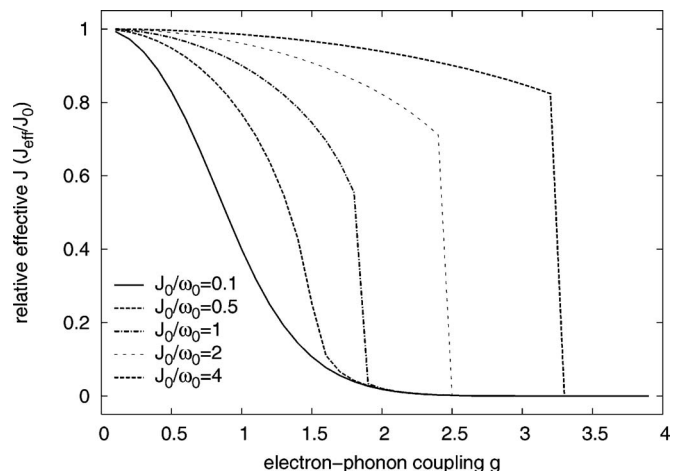


FIG. 5. Effective transfer integrals as a function of electron-phonon couplings g for systems with different bare transfer integrals J_0/ω_0 at low temperature ($\beta\omega_0=10$).

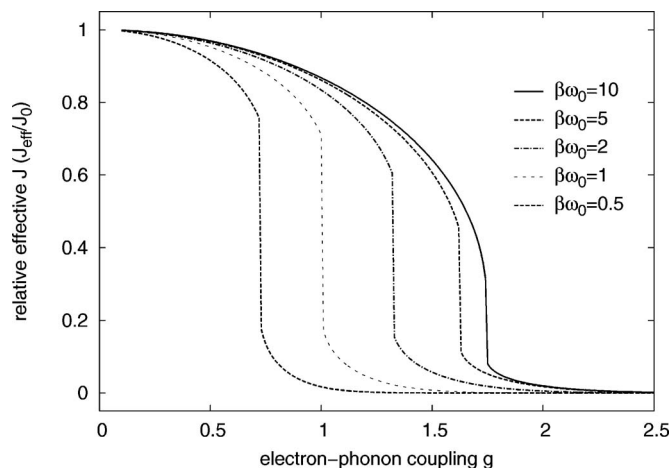


FIG. 6. Effective transfer integrals as a function of electron-phonon couplings g for a system with $J_0/\omega_0=0.8$ at different temperatures.

pling regime, signaling the small polaron transition. Note that at small J_0/ω_0 , the transition is smooth; however, for systems with sufficiently large J_0/ω_0 , the effective bandwidth changes abruptly. The abrupt change is due to the existence of two minima in the free energy functional with respect to the dressing coefficients. When a crossover of the free energies of the two minima occurs, the optimal set of variational parameters abruptly shifted from one minima to the other, resulting in a discontinuous change in the optimal polaron structure. Exact theorems on the ground state of the 1D Holstein model state that the adiabatic ground state energy and effective mass are analytical functions of the strength of electron-phonon coupling g ,^{24,60–62} and while the character of the polaron state can change sharply in a narrow g range, there is no true phase transition in this system. Allen and Silbey studied the abrupt change and showed that it is unphysical and due to the artifact of the variational method.^{24,32} In addition, a series of studies by Lindenberg *et al.* comparing a number of variational methods also clearly show that the abrupt change is due to the insufficient flexibility in the variational *ansatz*.^{37,39,42,48}

Figure 5 also shows that the critical coupling strength where the small polaron transition occurs depends on the reduced bare transfer integral J_0/ω_0 . For a narrow-band system whose J_0/ω_0 is small, the small polaron transition occurs at a smaller g , in contrast to wide-band systems with large J_0/ω_0 . This trend is the consequence of the competition between electronic coupling J_0 and electron-phonon coupling g . Note that different J_0/ω_0 can also be seen as different ω_0 . Given the same J_0 and electron-phonon coupling strength g , our theory predicts that higher frequency phonon modes tend to localize the electron, while the low frequency modes could only dress the electron weakly.

Evidence for band narrowing with the increase of temperature has been recently reported by Koch *et al.* for a pentacene thin film.¹⁴ Our finite-temperature variational method allows us to study the temperature dependence of the small polaron transition. In Fig. 6, we compare curves of the relative effective transfer integrals J_{eff}/J_0 at different temperatures for a system with $J_0/\omega_0=0.8$. While the asymptotic behaviors of J_{eff} at small $g \ll 1$ and large $g \gg 1$ are not tem-

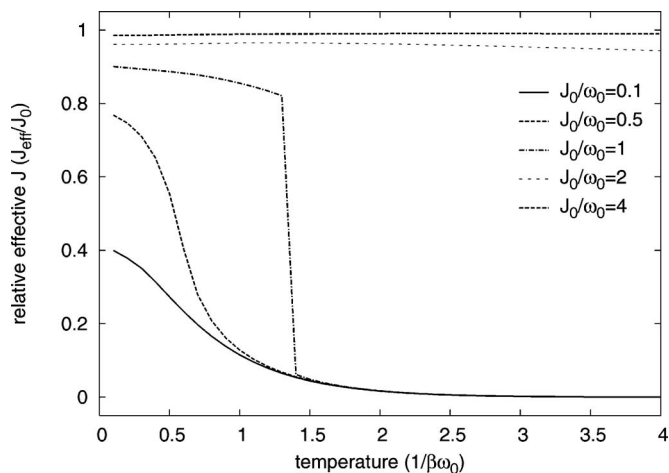


FIG. 7. Effective transfer integrals as a function of temperature for systems with $g=1$ and different bare transfer integrals. The small polaron transition signaled by a drop in J_{eff} is more dramatic for wide-band materials.

perature dependent, the transition point where J_{eff} sharply decreases depends on the temperature. At higher temperatures, the small polaron transition occurs at smaller g , and the abrupt change is more pronounced. In addition, Fig. 6 also indicates the polaronic (exponential) band narrowing effect at high temperatures.

Figure 7 shows the relative effective transfer integrals J_{eff}/J_0 as a function of the reduced temperature $1/\beta\omega_0$ for systems with $g=1$ and different bare transfer integrals. Clearly, the small polaron band narrowing factor $e^{-g^2 \coth(\beta\omega_0/2)}$ does not describe the temperature dependence in these intermediate coupling systems. The effective transfer integral J_{eff} is a complicated function of temperature because the variational parameters $\{f_m\}$ are also temperature dependent. Note that again a system with a larger bare transfer integral exhibits small polaron transition at a higher temperature. In the temperature range that we have shown in Fig. 7, the small polaron transition occurs smoothly at low temperatures for narrow-band materials whose reduced bare transfer integrals J_0/ω_0 are small. For a system with intermediate $J_0/\omega_0=1$, J_{eff} varies slowly at low temperature, and then drops suddenly at $1/\beta\omega_0 \sim 1.4$, indicating the appearance of an abrupt small polaron transition. For wide-band materials with large J_0/ω_0 , the effective transfer integrals J_{eff} are relatively temperature independent in the temperature range shown in Fig. 7; the abrupt transition to small polaron states for systems with $J_0/\omega_0 > 1.5$ occurs at higher temperatures not shown in the figure.

3. Phase diagrams

We summarize our findings about the characters of polaron states in the 1D Holstein model at different parameters in phase diagrams shown in Fig. 8. These phase diagrams map the character of the polaron state as a function of electron-phonon coupling constant g and reduced electronic transfer integral J_0/ω_0 at different temperatures. Regions of different polaron characters are labeled as L, L', S, S': L labels the region of large polaron states, S labels the region of small polaron states, L' labels the region where the free

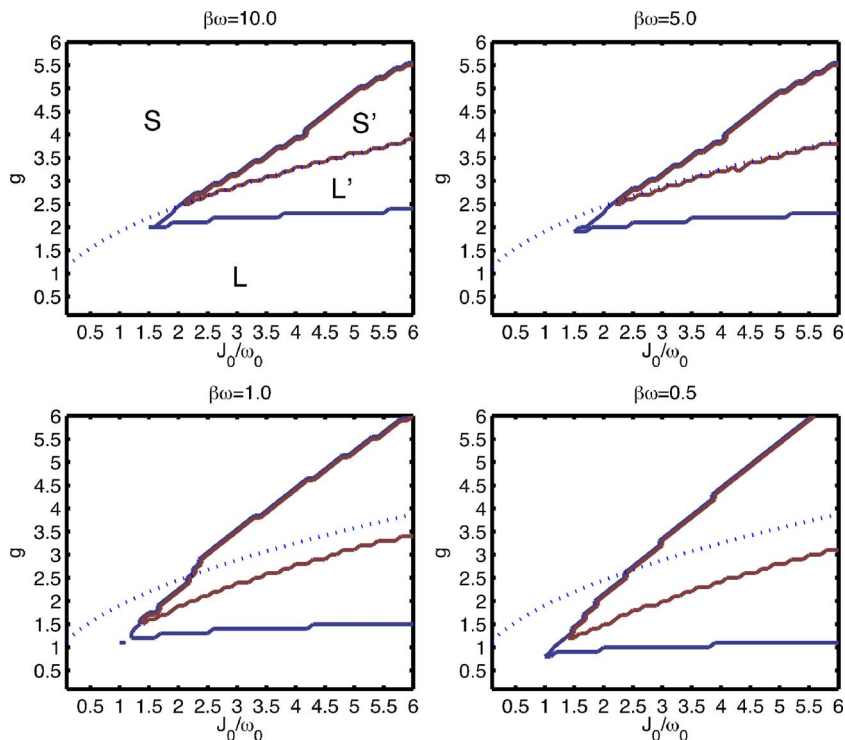


FIG. 8. (Color online) Polaron phase diagram determined using the finite-temperature variational method with Merrifield's *ansatz* at different temperatures. The dotted line is the empirical self-trapping line given by $g_{ST} = 1 + \sqrt{J_0/\omega_0}$.

energy functional A_0^e [Eq. (26)] exhibits spurious double minima with the lower A_0^e given by the large polaron state, and S' labels the region where spurious double minima exist and the small polaron state gives the lower A_0^e . In these phase diagrams, the wedge-shaped region includes states that exhibit double minima, and abrupt changes occur across the small polaron transition line separating the L' region and the S' region. For comparison, we also plotted an empirical self-trapping line that separates the small polaron region and the large polaron region of the 1D Holstein model at zero temperature,⁶³

$$g_{ST} = 1 + \sqrt{J_0/\omega_0}.$$

The self-trapping line is obtained by comparing the ground state energy from second-order WCPT and SCPT theories and is known to reproduce the critical points predicted by more accurate numerical methods. The excellent agreement between g_{ST} and the transition line predicted by our variational method at low temperatures indicates that our variational approach gives reasonable semiquantitative results at low temperatures. Although the abrupt transition due to spurious double minima is an artifact of the variational *ansatz*, it captures the point where the small polaron transition occurs.

Our finite-temperature variational method enables us to study the small polaron transition at finite temperatures and constructs phase diagrams at different temperatures (Fig. 8). As the temperature increases, the wedge-shaped region expands and the small polaron transition line marking the abrupt transition is shifted toward smaller g , indicating that the transition to small polaron states is assisted by thermal population of the phonon modes.

B. Bandlike and hopping mobilities

Figure 9 shows the results of our mobility calculations for a 1D nearest-neighbor system with reduced transfer integral $J_0/\omega_0=2$ and different electron-phonon coupling constants. The results clearly show universal band to hopping transitions in the mobilities, as observed in experiments. All theoretical curves exhibit a universal trend. The total mobility is temperature independent in extremely low temperatures because the mobility is determined by the additional scattering channel represented by γ_0 . After this impurity limited regime, the mobility decreases in a power-law fashion as the temperature increases. The steep power-law decrease continues over a wide temperature range, during which the mobility decreases by several orders of magnitudes. At intermediate to high temperatures, the mobility ceases to decrease and depends only weakly on the temperature. Eventually, an abrupt change in the mobility occurs at a high temperature, which corresponds to the abrupt transition to the small polaron state. Note that beyond this transition point, the polaron state is fully dressed and the polaron bandwidth is narrowed by an exponentially small factor, resulting in very different transport behavior after the transition. As we have mentioned, the abrupt change is unphysical and is an artifact of the Merrifield *ansatz*, therefore, mobility results around the discontinuity are questionable. Since the high temperature range in which the abrupt change occurs is usually not accessible in experiments, we disregard mobility points after the small polaron transition and focus on the transport properties of partially dressed states in this work.

In Fig. 9, we also show the bandlike contribution to the mobility as well as the hopping contribution. The total mobility is dominated by the bandlike term in low temperatures and by the hopping term in high temperatures. At low to intermediate temperatures, the bandlike term decreases

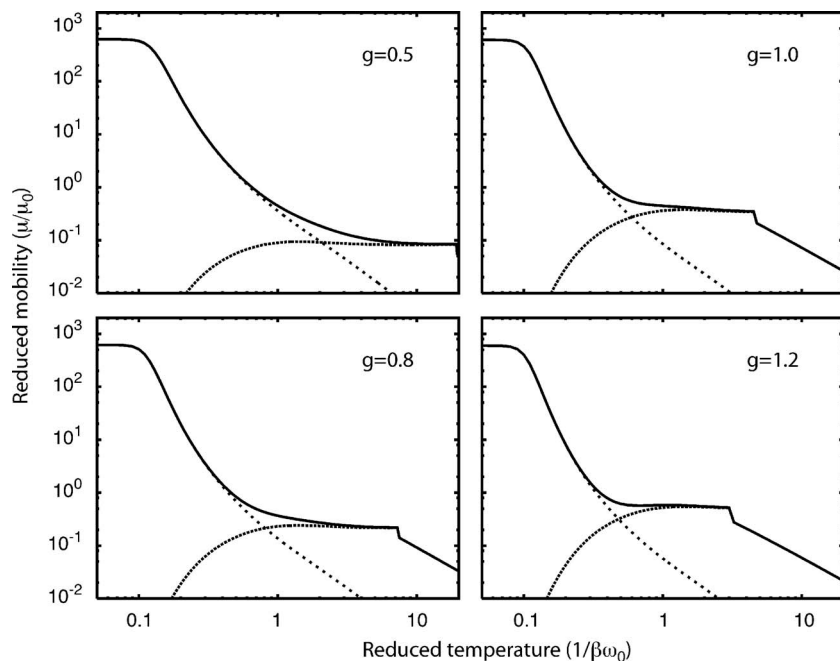


FIG. 9. Mobilities for a 1D Holstein system with $J_0/\omega_0=2$ at different electron-coupling constants g . We show the total mobility (solid lines), bandlike contribution to the mobility (thin dashed lines), and hopping contribution to the mobility (thick dashed lines). $\alpha=0.01\omega_0$ and $\gamma_0=0.001\omega_0$ are employed for these calculations. The unit of the y-axis is $\mu_0=ea_0^2/\hbar$, where e is the charge of an electron, a_0 is the lattice constant, and \hbar is Planck's constant.

monotonically, while the hopping term grows as temperature increases. At sufficiently high temperature, the hopping term dominates the mobility even when the electron is only weakly coupled to the phonons. The crossover of the bandlike and hopping terms results in the almost temperature independent mobility at the intermediate to high temperature regime. Note that the crossover temperature T_c where the crossover from bandlike to hopping transport occurs depends on J_0/ω_0 and g . In general, a weak-coupling (small g) or wide-band (large J_0/ω_0) system has higher T_c .

To study how the strength of electron-phonon coupling g affects the mobility, we compare the bandlike and hopping mobilities for a 1D Holstein system with $J_0/\omega_0=2$ at different electron-coupling constants (Fig. 10). The comparison shows that varying the strength of electron-phonon coupling has different effects on the bandlike term and the hopping term. Because an increase in g results in more scattering of the polaron state, the hopping mobility (high- T) is enhanced by strong electron-phonon couplings, while the bandlike mobility (low- T) is inhibited. Notice that varying g could result in a change of mobility over several orders of magnitude. Thus, our results suggest that selecting a material with proper g value is important for optimizing charge-carrier mobilities at different temperatures; given the same reduced transfer integral J_0/ω_0 , small g materials are favorable at low temperatures (higher bandlike mobility), while large g materials are favorable at high temperatures (higher hopping mobility). Note that this result is valid only when the system is still described by a partially dressed state. After the abrupt small polaron transition, the exponential renormalization of the transfer integrals (band narrowing effect) will dominate the g dependence of the charge-carrier mobility. Therefore, after the small polaron transition, increasing g will lower the mobility.

In a number of previous studies, the small polaron transition in a variational treatment is considered to correspond to the crossover from the bandlike to hopping transport.^{13,31}

However, our results suggest that the two phenomena are not directly correlated. The smooth crossover in the transport mechanisms does not correspond to the transition in the structure of the polaron state; in contrast, the crossover from

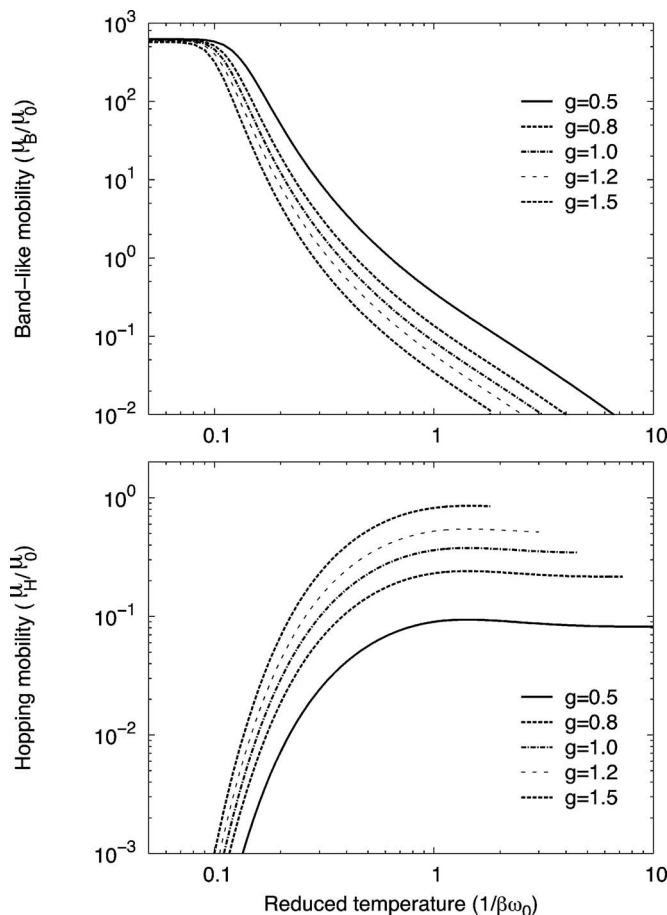


FIG. 10. A comparison of bandlike (upper panel) and hopping (lower panel) mobilities for a 1D Holstein system with $J_0/\omega_0=2$ at different electron-coupling constants.

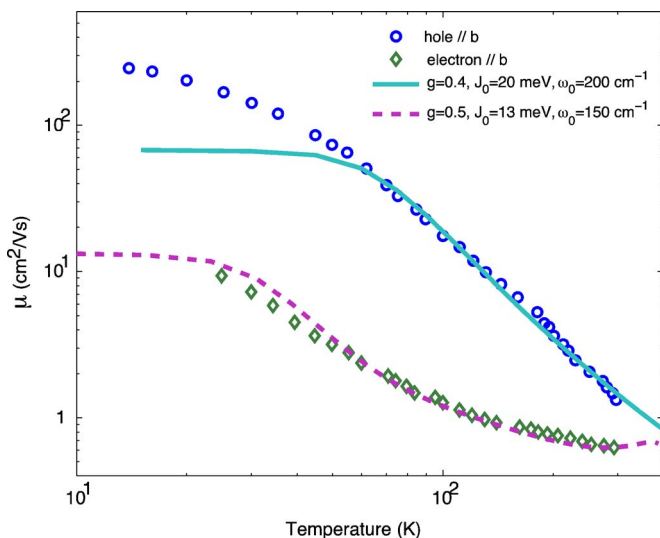


FIG. 11. (Color online) A comparison of our results with experimental measurements on ultrapure naphthalene crystals. Both excess electron and hole mobilities measured in parallel to the crystalline b direction of the naphthalene crystals are shown alongside with selected 1D results from our theory presented in the previous section. In addition, $\gamma_0=0.025\omega_0$ and $\alpha=0.05\omega_0$ are employed in the numerical calculations.

the bandlike mechanism to the hopping mechanism occurs at a lower temperature compared to the small polaron transition (the abrupt change in the mobilities). Our results indicate that partially dressed state can give rise to a significant hopping term in a broad parameter range, which may be responsible for the bandlike to hopping transition observed in experiments

We summarize key qualitative results that are exhibited by our partially dressed theory: (1) A steep power-law decrease of the mobility exists in the bandlike regime, and the $n > 1.5$ behavior can be explained by the contribution from the multiphonon scattering in the bandlike term; (2) all theoretical curves predict smooth bandlike to hopping transition in the temperature dependence of charge-carrier mobilities; however, the change in transport mechanism does not correspond to the small polaron transition; (3) almost temperature independent behavior over a wide temperature range exists in some parameter regime; (4) significant thermal-activated mobility at high temperature is not observed in all parameter regimes that we have studied; however, for sufficiently strong electron-phonon couplings, a slight increase in the mobility can occur after the crossover from the bandlike to hopping transport.

V. TEMPERATURE DEPENDENCE ON THE CHARGE MOBILITIES IN NAPHTHALENE

We also compare our mobility calculations to experimental measurements of excess charge-carrier mobilities on the naphthalene crystals. In Fig. 11, we compare two theoretical curves from the 1D model presented in the previous section to excess electron and hole mobilities measured in parallel to the crystalline b direction of the naphthalene

crystals.^{5,64} The curves with $(g, J_0, \omega_0) = (0.4, 20 \text{ meV}, 200 \text{ cm}^{-1})$ and $(0.5, 13 \text{ meV}, 150 \text{ cm}^{-1})$ are in agreement with experimental excess hole and electron mobilities, respectively. The fitting parameters indicate weak electron-phonon couplings and are consistent with other spectroscopic experiments^{65–69} and theoretical calculations^{70–72} on naphthalene crystals.

Our simplified 1D model is hardly adequate for the description of the mobility in naphthalene crystal because of the highly anisotropic and noncubic structure of the crystal. Using the theoretical model presented in Sec. II, it is possible to construct a three dimensional (3D) description that takes into account the real crystal structure; however, such complete simulation would be beyond the scope of this work. Figure 11 is not meant to provide a fit to the experimental data. Nevertheless, it demonstrates that our approach does capture the temperature dependence of the mobilities and can provide a quantitative description that covers the whole experimental temperature range and different types of materials in a unified theory.

VI. CONCLUDING REMARKS

In conclusion, we have developed a unified theory that describes both coherent and incoherent transports in the Holstein Hamiltonian and can quantitatively describe the temperature dependence of the charge-carrier mobilities in OMC. Our formalism is based on a finite-temperature variational method combining Merrifield's transformation with Bogoliubov's theorem to obtain the optimal basis for an interacting electron-phonon system, and then to calculate the bandlike and hopping mobilities for charge carriers based on the optimal basis. Because we use Bogoliubov's theorem to obtain the optimal thermal mean-field description for the interacting electron-phonon system, a perturbation expansion based on the variational zeroth-order Hamiltonian is justified in the intermediate coupling regime. Our calculations on the 1D Holstein model at $T=0$ K and finite temperatures indicate that the variational-perturbation method gives results that compared favorably to other analytical methods.

Moreover, we have applied the unified theory to the 1D Holstein model at finite temperatures. We studied the structures of polaron states over a broad range of parameters including different temperatures. Our method yields phase diagrams that are in agreement with predictions of more accurate numerical methods at low temperatures. Therefore, the finite-temperature Merrifield's variational method, although contains unphysical double minima on the free energy potential surface, gives reasonable semiquantitative results for the polaron transition. We also calculated the bandlike and hopping mobilities of the 1D model in different parameters and showed that the temperature dependence of the total mobility predicted by our theory exhibits power-law decay at a wide temperature range, and an almost temperature independent behavior at higher temperatures before an abrupt change occurs. We found that as the temperature

increases, the hopping transport can become dominant character even before the polaron state changes its characters. Thus, our result indicates that the self-trapping transition studied in conventional polaron theories does not necessary correspond to the crossover from bandlike to hopping transport in the transport properties in OMC. Comparing our 1D results with experiments on ultrapure naphthalene crystals suggests that our method can describe the charge-carrier mobilities in OMC quantitatively across the whole experimental temperature range.

Although our variational method correctly predicts the small polaron transition line at low temperatures, the abrupt transition makes it difficult to access regions close to or after the transition quantitatively. A more generalized *ansatz*, such as Toyozawa's *ansatz*, should greatly improve the applicable range of the current theory. Note that our results suggest that the crossover from bandlike to hopping transport occurs *before* the self-trapping transition, thus, the deficiency does not affect our main results regarding the charge-carrier mobilities in OMC.

Finally, we note that the mobility expression from Yarkony and Silbey [Eqs. (A5)–(A8)] is an approximate expression in which small terms have been dropped. Since we have used numerical integration to evaluate the mobilities, it is straightforward to numerically propagate the reduced density matrix of the system according to the master equation in Eq. (A2), and then calculate the mobility using Eq. (A4). Such direct propagation scheme is favorable when simulating real 3D systems because numerical integration of 3D functions is not efficient. In addition, static disorders and nonequilibrium effect can be easily incorporated into such a numerical scheme, making the approach favorable when modeling disorder materials.

ACKNOWLEDGMENTS

This research was supported by the NSF Grant No. CHE0556268.

APPENDIX A: EXPRESSION FOR MOBILITY CALCULATIONS

Yarkony and Silbey considered a general electron-phonon Hamiltonian,

$$H = H_e + H_{ph} + V$$

$$= \sum_k E_k a_k^\dagger a_k + \sum_q \omega_q b_q^\dagger b_q + \frac{1}{\sqrt{N}} \sum_{k_1, k_2} a_{k_1}^\dagger a_{k_2} V_{k_1 k_2}, \quad (\text{A1})$$

where $V_{k_1 k_2}$ are operators that act on phonon degrees of freedom. Using a quantum master equation approach in a approximation equivalent to second-order time-dependent perturbation theory in the exciton-phonon coupling V , they find the equation of motion for the reduced density matrix of the exciton,

$$\dot{\sigma}_{kk'}(t) = -i(E_k - E_{k'})\sigma_{kk'}(t) - \Gamma_{kk'}\sigma_{kk'}(t) + \sum_{q,s} W_{kk';qs}\sigma_{qs}(t), \quad (\text{A2})$$

where E_k is the energy of the state k , the relaxation tensor $W_{kk';qq'}$ is defined using phonon correlation functions

$$W_{kk';qq'} = \int_0^\infty d\tau \{ \langle V_{q'k'}(\tau) V_{kq}(\tau) \rangle_0 e^{-i(E_{q'} - E_k)\tau} + \langle V_{q'k'}(\tau) V_{kq} \rangle_0 e^{-i(E_k - E_{q'})\tau} \}, \quad (\text{A3})$$

and the quantities $\Gamma_{kk'}$ is given by

$$\Gamma_{kk'} = \frac{1}{2} \sum_q (W_{qq;kk} + W_{qq;k'k'}).$$

Note that the diffusion coefficient D of a nonequilibrium distribution of electronic states can be related to the mean-square displacement of a particle $\langle R^2(t) \rangle$ using the following expression:

$$D = \frac{1}{2d} \lim_{t \rightarrow \infty} \frac{d}{dt} \langle R^2(t) \rangle,$$

where d is the dimensionality of the system (assuming an isotropic system). The mean-square displacement of a particle is related to the diagonal density matrix elements of the system in the site representation, $\langle R^2(t) \rangle = \sum_n n^2 \sigma_{nn}(t)$. In the k -representation, the diffusion coefficient is given by

$$D = \frac{1}{2d} \lim_{t \rightarrow \infty} \sum_k \nabla_k^2 \dot{\sigma}_{k,k+k}(t) |_{K=0}. \quad (\text{A4})$$

Substitution of the quantum master equation in Eq. (A2) into this equation in the limit of $t \rightarrow \infty$ yields a complicated equation that gives the diffusion coefficient of the electron. After neglecting small terms, an approximate formula for the mobility of the electron that consists of a bandlike term and a hopping term is obtained,

$$\mu = e\beta D = \mu_B + \mu_H, \quad (\text{A5})$$

where the bandlike mobility is given by

$$\mu_B = e\beta \sum_k \sigma_{kk}^{\text{eq}} \cdot \frac{v_k^2}{\gamma_0 + \Gamma_{kk}}, \quad (\text{A6})$$

where e is the electron charge, $\sigma_{kk}^{\text{eq}} = e^{-\beta E_k} / \sum_q e^{-\beta E_q}$ is the thermal population of state k , $v_k = \nabla_k E_k$ is the electron group velocity in state k , Γ_{kk} is the rate of scattering out of state k ,

$$\Gamma_{kk} = \sum_q W_{qq;kk},$$

and γ_0 is an extra term inserted to represent the contribution to the scattering rate from mechanisms not considered in the Hamiltonian (e.g., scattering due to quadratic electron-phonon couplings and impurities).

The hopping term is given by

$$\mu_H = e\beta \sum_k \sigma_{kk}^{\text{eq}} \cdot \gamma_{kk}, \quad (\text{A7})$$

where γ_{kk} is a function defined using the relaxation tensor W ,

$$\gamma_{kk} = -\operatorname{Re} \sum_q \left. \frac{d^2 W_{q,q+K;k,k+K}}{dK^2} \right|_{K=0} + \frac{1}{2} \frac{d^2 \Gamma_{kk}}{dk^2}. \quad (\text{A8})$$

Equations (A5)–(A8) are the main results derived by Yarkony and Silbey. We will adopt their expression to calculate the mobility of a partially dressed electron governed by the transformed Hamiltonian in Eq. (7).

We first evaluate the phonon correlation functions $\langle V_{q'k'} V_{kq}(\tau) \rangle_0$. Reorganizing the interaction term of the transformed Hamiltonian in Eq. (8) and comparing the result to Eq. (A1), we obtain the corresponding phonon operators for the Hamiltonian after Merrifield's transformation,

$$V_{k_1 k_2} = \frac{1}{N} \sum_{n,m} e^{-ik_1 n} e^{ik_2 m} \cdot J_{n,m} \cdot (\theta_n^\dagger \theta_m - \langle \theta_n^\dagger \theta_m \rangle_0) + \omega_0 (g - f_{k_1 - k_2}) \cdot (b_{k_1 - k_2} + b_{k_2 - k_1}^\dagger). \quad (\text{A9})$$

This expression for phonon operators is used to compute the phonon correlation functions $\langle V_{q'k'} V_{kq}(\tau) \rangle_0$. Due to the com-

plex form of $V_{k_1 k_2}$, the expression for $\langle V_{q'k'} V_{kq}(\tau) \rangle_0$ is quite involved; to avoid confusion, the result is given in Appendix B.

Our mobility calculations depend on the evaluation of the following relaxation tensor elements:

$$W_{q,q+K;k,k+K} = \int_0^\infty d\tau \{ \langle V_{k+K,q+K} V_{qk}(\tau) \rangle_0 e^{-i(E_{k+K} - E_{q+K})\tau} + \langle V_{k+K,q+K}(\tau) V_{qk} \rangle_0 e^{-i(E_q - E_k)\tau} \}.$$

In order to evaluate the integral over τ while avoiding singularities introduced by δ functions, we assume a phonon bandwidth α (inverse relaxation time of phonons) and treat integral of the form $\operatorname{Re} \int d\tau e^{iF\tau}$ as

$$\operatorname{Re} \int_0^\infty d\tau e^{iF\tau} \cdot e^{-\alpha\tau} = \frac{\alpha}{\alpha^2 + F^2}.$$

The result for $W_{q,q+K;k,k+K}$ is

$$W_{q,q+K;k,k+K} = n_0 \omega_0^2 (g^2 - f_{k-q}^2) \left[\frac{\alpha}{\alpha^2 + (\varepsilon_q - \varepsilon_k - \omega_0)^2} + \frac{\alpha}{\alpha^2 + (\varepsilon_{q+K} - \varepsilon_{k+K} - \omega_0)^2} \right] + (n_0 + 1) \omega_0^2 (g^2 - f_{k-q}^2) \times \left[\frac{\alpha}{\alpha^2 + (\varepsilon_q - \varepsilon_k + \omega_0)^2} + \frac{\alpha}{\alpha^2 + (\varepsilon_{q+K} - \varepsilon_{k+K} + \omega_0)^2} \right] + \frac{1}{N} \sum_{n_1, m_1} \sum_{n_2, m_2} e^{-ik(n_1 - m_2)} e^{-iq(n_2 - m_1)} \tilde{J}_{n_1 m_1} \tilde{J}_{n_2 m_2} \times \sum_{n=1}^\infty \sum_{m=0}^n \frac{A^m B^{n-m}}{m!(n-m)!} \times \left\{ \frac{\alpha}{\alpha^2 + [\varepsilon_q - \varepsilon_k + (2m-n)\omega_0]^2} + \frac{\alpha}{\alpha^2 + [\varepsilon_{q+K} - \varepsilon_{k+K} + (2m-n)\omega_0]^2} \right\}, \quad (\text{A10})$$

where we have defined thermal population number of phonon modes $n_0 = 1/(e^{-\beta\omega_0} - 1)$, phonon renormalized resonance transfer integrals $\tilde{J}_{nm} = J_{nm} \langle \theta_n^\dagger \theta_m \rangle_0$, and functions

$$A = \frac{-1}{2} \sum_{q'} X_{q'}^{n_1 m_1} \bar{X}_{q'}^{n_2 m_2} \cdot (n_0 + 1),$$

$$B = \frac{-1}{2} \sum_{q'} \bar{X}_{q'}^{n_1 m_1} X_{q'}^{n_2 m_2} \cdot n_0,$$

with $X_q^{nm} = (1/\sqrt{N}) f_q(e^{iqm} - e^{iqn})$ and $\bar{X}_q^{nm} = (1/\sqrt{N}) f_q^*(e^{-iqm} - e^{-iqn})$. Note that for narrow phonon bands, the value for α should be small ($0 < \alpha \ll 1$), and when $\alpha \rightarrow 0$ we obtain δ functions in the expression.

The three terms in Eq. (A10) have simple physical interpretations. The first term represents a process in which an electron absorbs one phonon and is scattered upward to a higher energy state, the second term is a process that emits a phonon and scatters the electron downward to a lower energy state, and the third term represents multiphonon processes in which multiple phonons are exchanged. For very narrow-band materials whose electronic bandwidth is smaller than

the phonon frequency ω_0 , only the multiphonon term contributes to the scattering of electrons. In addition, for systems with strong electron-phonon coupling g , it is possible that at high temperatures, the polaronic narrowing effect will result in a narrow polaron band such that $\tilde{J} \ll \omega$, and again the single phonon processes (the first and second terms) do not contribute. Note that at low temperatures ($n_0 \ll 1$) or when the electron is only weakly dressed ($f_m \ll 1$), the prefactor $A^m B^{n-m} \ll 1$ and the multiphonon processes are negligible. On the other hand, when temperature increases, the thermal population of phonon modes n_0 as well as the dressing coefficients $\{f_m\}$ increases, and the contribution of the multiphonon term would increase. Eventually, multiphonon term dominates the scattering of electrons at high temperatures.

APPENDIX B: PHONON CORRELATION FUNCTIONS

The phonon correlation function $\langle V_{q'k'} V_{kq}(\tau) \rangle_0$ for a narrow phonon band with phonon frequency ω_0 is given by

$$\begin{aligned} \langle V_{q'k'} V_{kq}(\tau) \rangle_0 &= \frac{1}{N} \sum_{n_1, m_1} \sum_{n_2, m_2} e^{-iq'n_1} e^{ik'm_1} e^{-ikn_2} e^{iqm_2} \tilde{J}_{n_1 m_1} \tilde{J}_{n_2 m_2} \times \{ e^{-\sum_s [X_s^{n_1 m_1} \bar{X}_s^{n_2 m_2} (n_0+1) e^{i\omega_0 \tau} + \bar{X}_s^{n_1 m_1} X_s^{n_2 m_2} n_0 e^{-i\omega_0 \tau}] - 1} \} + \frac{\omega_0}{N} (g \\ &- f_{k-q}) \sum_{n, m} e^{-iq'n} e^{ik'm} \tilde{J}_{nm} \bar{X}_{k-q}^{nm} [-n_0 e^{-i\omega_0 \tau} + (n_0+1) e^{i\omega_0 \tau}] + \frac{\omega_0}{N} (g - f_{q'-k'}) \sum_{n, m} e^{-ikn} e^{iqm} \tilde{J}_{nm} \bar{X}_{q'-k'}^{nm} [n_0 e^{-i\omega_0 \tau} - (n_0 \\ &+ 1) e^{i\omega_0 \tau}] + \omega_0^2 (g - f_{q'-k'})^2 \cdot [n_0 e^{-i\omega_0 \tau} + (n_0+1) e^{i\omega_0 \tau}] \cdot \delta(q' - k' + k - q), \end{aligned}$$

where we have defined $\tilde{J}_{nm} = J_{nm} \langle \theta_n^\dagger \theta_m \rangle_0$, $X_q^{nm} = (1/\sqrt{N}) f_q (e^{iqm} - e^{iqn})$, $\bar{X}_q^{nm} = (1/\sqrt{N}) f_q^* (e^{-iqm} - e^{-iqn})$, and $n_0 = 1/(e^{-\beta\omega_0} - 1)$. Note that using the symmetry property of quantum correlation functions, we can easily calculate the other correlation function $\langle V_{q'k'}(\tau) V_{kq} \rangle_0$,

$$\langle V_{q'k'}(\tau) V_{kq} \rangle_0 = \langle V_{q'k'} V_{kq}(\tau) \rangle_0^*.$$

APPENDIX C: SECOND-ORDER CORRECTION ON THE ENERGY BAND AT $T=0$ K

The second-order energy correction to the energy band of the polaron state in Eq. (17) assumes the following form:

$$\begin{aligned} E^{(2)}(k) &= -2\omega_0 f_{\text{opt}}(g - f_{\text{opt}}) - \omega_0^2 (g^2 - f_{\text{opt}}^2) \frac{1}{N} \sum_{k'} \frac{1}{2\tilde{J}_0 \cos k' - 2\tilde{J}_0 \cos k - \omega_0} \\ &- 2\tilde{J}_0^2 \sum_{n_T=1}^{\infty} \frac{f_{\text{opt}}^{2n_T}}{n_T!} \frac{1}{N} \sum_{k'} \frac{2^{n_T} + \cos 2k + \cos 2k' + 2 \cdot (-1)^{n_T} \cos(k' - k) + (-2)^{n_T} \cos(k' + k)}{2\tilde{J}_0 \cos k' - 2\tilde{J}_0 \cos k - n_T \omega_0}, \end{aligned}$$

where we have defined $\tilde{J}_0 = J_0 e^{-f_{\text{opt}}}$. Around the bottom of the band where $k \sim 0$ and $\cos k \sim 1$, the integral over k' can be evaluated explicitly to give

$$\begin{aligned} E_{k \sim 0}^{(2)}(k) &= -2\omega_0 f_{\text{opt}}(g - f_{\text{opt}}) - \omega_0^2 (g^2 - f_{\text{opt}}^2) \\ &\times \frac{1}{2\tilde{J}_0 \sqrt{(\cos k + \omega_0/2\tilde{J}_0)^2 - 1}} - 2\tilde{J}_0 \sum_{n_T=1}^{\infty} \frac{f_{\text{opt}}^{2n_T}}{n_T!} \\ &\times \frac{A\sqrt{A^2 - 1} - AB + B\sqrt{A^2 - 1} - A^2 - C}{\sqrt{A^2 - 1}}, \quad (\text{C1}) \end{aligned}$$

where the auxiliary functions are defined as

$$A = \cos k + n_T \omega_0 / 2\tilde{J}_0,$$

$$B = \frac{1}{2} [2(-1)^{n_T} + (-2)^{n_T}] \cos k,$$

$$C = \frac{1}{2} [2^{n_T} + \cos 2k - 1].$$

The expression for $E_{k \sim 0}^{(2)}(k)$ is used to calculate the effective mass of the polaron state at $T=0$ K.

¹M. Pope and C. E. Swenberg, *Electronic Processes in Organic Crystals* (Oxford University Press, New York, 1982).

²N. Karl, *J. Vac. Sci. Technol. A* **17**, 2318 (1999).

³*Organic Electronic Materials: Conjugated Polymers And Low Molecular Weight Organic Solids*, edited by R. Farchioni and G. Grosso (Springer, New York, 2001).

⁴V. Coropceanu, J. Cornil, D. A. da Silva Filho, Y. Olivier, R. J. Silbey, and J.-L. Brédas, *Chem. Rev. (Washington, D.C.)* **107**, 926 (2007).

⁵N. Karl, *Organic Semiconductors*, Landolt Börnstein/New Series Group III Vol. 17 (Springer, Berlin, 1985), Subvol. 17i, pp. 106–218.

⁶N. Karl, *Mol. Cryst. Liq. Cryst.* **171**, 31 (1989).

⁷N. Karl, *J. Cryst. Growth* **99**, 1009 (1990).

⁸C. E. Swenberg and M. Pope, *Chem. Phys. Lett.* **287**, 535 (1998).

⁹E. A. Silinsh and V. Čápek, *Organic Molecular Crystals: Interaction, Localization, and Transport Phenomena* (AIP, Woodbury, 1994).

¹⁰M. E. Gershenson, V. Podzorov, and A. F. Morpurgo, *Rev. Mod. Phys.* **78**, 973 (2006).

¹¹J. Zaumseil and H. Siringhaus, *Chem. Rev. (Washington, D.C.)* **107**, 1296 (2007).

¹²Y. C. Cheng, R. J. Silbey, D. A. da Silva, J. P. Calbert, J. Cornil, and J. L. Bredas, *J. Chem. Phys.* **118**, 3764 (2003).

¹³P. E. Parris and V. M. Kenkre, *Phys. Rev. B* **70**, 064304 (2004).

¹⁴N. Koch, A. Vollmer, I. Salzmann, B. Nickel, H. Weiss, and J. Rabe, *Phys. Rev. Lett.* **96**, 156803 (2006).

¹⁵R. M. Glaeser and R. S. Berry, *J. Chem. Phys.* **44**, 3797 (1966).

¹⁶H. Haken and G. Strobl, *Z. Phys.* **262**, 135 (1973).

¹⁷H. Haken and P. Reineker, *Z. Phys.* **249**, 253 (1972).

¹⁸P. Reineker, *Exciton Dynamics in Molecular Crystals and Aggregates* (Springer-Verlag, Berlin, 1982).

¹⁹V. Čápek, *Chem. Phys.* **171**, 79 (1993).

²⁰A. Troisi and G. Orlandi, *Phys. Rev. Lett.* **96**, 086601 (2006).

²¹M. Hultell and S. Stafstrom, *Chem. Phys. Lett.* **428**, 446 (2006).

²²B. Jackson and R. J. Silbey, *J. Chem. Phys.* **75**, 3293 (1981).

²³T. Holstein, *Ann. Phys. (N.Y.)* **8**, 325 (1959).

²⁴D. Emin, *Adv. Phys.* **22**, 57 (1973).

²⁵D. R. Yarkony and R. J. Silbey, *J. Chem. Phys.* **67**, 5818 (1977).

²⁶R. J. Silbey and R. W. Munn, *J. Chem. Phys.* **72**, 2763 (1980).

²⁷R. W. Munn and R. Silbey, *Mol. Cryst. Liq. Cryst.* **57**, 131 (1980).

²⁸V. M. Kenkre, J. D. Andersen, D. H. Dunlap, and C. B. Duke, *Phys. Rev. Lett.* **62**, 1165 (1989).

²⁹S. Rackovsky and R. Silbey, *Mol. Phys.* **25**, 61 (1973).

³⁰J. D. Andersen, C. B. Duke, and V. M. Kenkre, *Chem. Phys. Lett.* **110**, 504 (1984).

³¹D. R. Yarkony and R. J. Silbey, *J. Chem. Phys.* **65**, 1042 (1976).

³²J. W. Allen and R. Silbey, *J. Chem. Phys.* **43**, 341 (1979).

³³T. Holstein, *Ann. Phys. (N.Y.)* **8**, 343 (1959).

³⁴R. W. Munn and R. Silbey, *J. Chem. Phys.* **83**, 1843 (1985).

³⁵R. W. Munn and R. Silbey, *J. Chem. Phys.* **83**, 1854 (1985).

³⁶R. E. Merrifield, *J. Chem. Phys.* **40**, 445 (1964).

³⁷Y. Zhao, D. W. Brown, and K. Lindenberg, *J. Chem. Phys.* **106**, 5622 (1997).

³⁸Y. Toyozawa, *Prog. Theor. Phys.* **26**, 29 (1961).

³⁹D. W. Brown, K. Lindenberg, and Y. Zhao, *J. Chem. Phys.* **107**, 3179 (1997).

- ⁴⁰J. Bonca, S. A. Trugman, and I. Batistic, *Phys. Rev. B* **60**, 1633 (1999).
- ⁴¹L. C. Ku, S. A. Trugman, and J. Bonca, *Phys. Rev. B* **65**, 174306 (2002).
- ⁴²A. H. Romero, D. W. Brown, and K. Lindenberg, *J. Chem. Phys.* **109**, 6540 (1998).
- ⁴³H. De Raedt and A. Lagendijk, *Phys. Rev. B* **27**, 6097 (1983).
- ⁴⁴H. De Raedt and A. Lagendijk, *Phys. Rev. B* **30**, 1671 (1984).
- ⁴⁵G. Kopidakis, C. M. Soukoulis, and E. N. Economou, *Phys. Rev. B* **51**, 15038 (1995).
- ⁴⁶E. V. L. de Mello and J. Ranninger, *Phys. Rev. B* **58**, 14625 (1998).
- ⁴⁷C. L. Zhang, E. Jeckelmann, and S. R. White, *Phys. Rev. B* **60**, 14092 (1999).
- ⁴⁸Y. Zhao, D. W. Brown, and K. Lindenberg, *J. Chem. Phys.* **107**, 3159 (1997).
- ⁴⁹E. Jeckelmann and S. R. White, *Phys. Rev. B* **57**, 6376 (1998).
- ⁵⁰A. S. Alexandrov, V. V. Kabanov, and D. K. Ray, *Phys. Rev. B* **49**, 9915 (1994).
- ⁵¹M. K. Grover and R. Silbey, *J. Chem. Phys.* **52**, 2099 (1970).
- ⁵²M. Grover and R. Silbey, *J. Chem. Phys.* **54**, 4843 (1971).
- ⁵³F. Marsiglio, *Physica C* **244**, 21 (1995).
- ⁵⁴E. I. Rashba, *Excitons* (North-Holland, Amsterdam, 1982), p. 543.
- ⁵⁵P. O. J. Scherer, E. W. Knapp, and S. F. Fischer, *Chem. Phys. Lett.* **106**, 191 (1984).
- ⁵⁶K. S. Song and R. T. Williams, *Self-Trapped Excitons* (Springer-Verlag, Berlin, 1993).
- ⁵⁷G. Wellein and H. Fehske, *Phys. Rev. B* **58**, 6208 (1998).
- ⁵⁸A. H. Romero, D. W. Brown, and K. Lindenberg, *J. Lumin.* **83**, 147 (1999).
- ⁵⁹D. W. Brown, A. H. Romero, and K. Lindenberg, *J. Phys. Chem. A* **103**, 10417 (1999).
- ⁶⁰D. Emin and T. Holstein, *Phys. Rev. Lett.* **36**, 323 (1976).
- ⁶¹H. Löwen, *J. Math. Phys.* **29**, 1505 (1988).
- ⁶²B. Gerlach and H. Löwen, *Rev. Mod. Phys.* **63**, 63 (1991).
- ⁶³A. H. Romero, D. W. Brown, and K. Lindenberg, *Phys. Rev. B* **60**, 4618 (1999).
- ⁶⁴L. B. Schein, W. Warta, A. R. McGhie, and N. Karl, *Chem. Phys. Lett.* **100**, 34 (1983).
- ⁶⁵E. L. Bokhenkov, I. Natkanets, and E. F. Sheka, *Zh. Eksp. Teor. Fiz.* **70**, 1027 (1976).
- ⁶⁶B. Dorner, E. L. Bokhenkov, E. F. Sheka, S. L. Chaplot, G. S. Pawley, J. Kalus, U. Schmelzer, and I. Natkaniec, *J. Phys. Colloq.* **42**, (C6)-602 (1981).
- ⁶⁷E. L. Bokhenkov, A. I. Kolesnikov, T. A. Krivenko, E. F. Sheka, V. A. Dementjev, and I. Natkaniec, *J. Phys. Colloq.* **42**, (C6)-605 (1981).
- ⁶⁸N. Sato, H. Inokuchi, B. M. Schmid, and N. Karl, *J. Chem. Phys.* **83**, 5413 (1985).
- ⁶⁹A. L. Motyka, S. A. Wittmeyer, R. J. Babbitt, and M. R. Topp, *J. Chem. Phys.* **89**, 4586 (1988).
- ⁷⁰V. Coropceanu, M. Malagoli, D. A. da Silva Filho, N. E. Gruhn, T. G. Bill, and J. L. Brédas, *Phys. Rev. Lett.* **89**, 275503 (2002).
- ⁷¹T. Kato and T. Yamabe, *J. Chem. Phys.* **115**, 8592 (2001).
- ⁷²T. Kato, M. Kondo, K. Yoshizawa, and T. Yamabe, *Synth. Met.* **126**, 75 (2002).
- ⁷³W. Stephan, *Phys. Rev. B* **54**, 8981 (1996).